Experimental investigations of the topology of spatially random systems

Asymptotic results for Betti numbers of Poisson points

Phys Rev E (2006)

Percolating length scales in persistence diagrams from porous materials

Water Resources Research (2015)

Vanessa Robins

Applied Mathematics

RSPE, ANU

Canberra, Australia

ARC Discovery Projects
DP0666442
DP1101028
ARC Future Fellowship
FT140100604

Part 1 Outline

- Betti numbers of spheres centered on point patterns, as a refinement of results for the Euler characteristic from Stochastic and Integral Geometry
  - eg texts by Stoyan, Kendall, Mecke. Schneider and Weil.
- Alpha shapes and the incremental Betti number algorithm
  - Delfinado and Edelsbrunner, 1993.
- The distribution of Poisson Delaunay Cell shapes
  - (Miles, 1974. Muche, 1996, 1998. Also the Okabe Boots Sugihara Chiu book)
- Asymptotic expressions for the Betti numbers of Poisson points in the low intensity limit
  - (Quintanilla and Torquato, 1996. VR 2006)

Australian National University

Tools for studying structure in point patterns

- Look at how something varies with distance
- something might be:
  - Number of points in shell of radius r (two pt correlation fn)
  - Minkowski functionals

    (volume, surface area, mean curvature, Euler characteristic)
  - Connected components (continuum percolation)
  - Betti numbers (higher-order topological measures)

In 3D: β_0 is number of components

β_1 is number of independent, non-contractible loops

β_2 is number of enclosed voids

Voronoi diagram

Delaunay triangulation

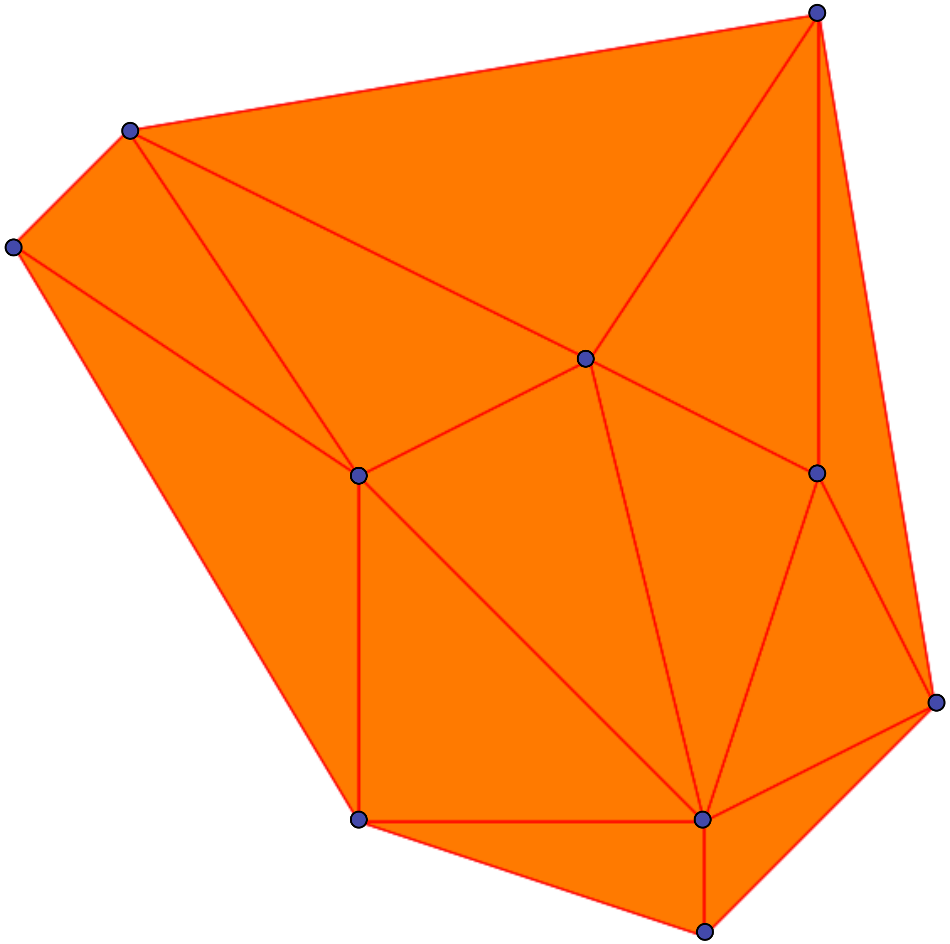

Union of balls, radius α

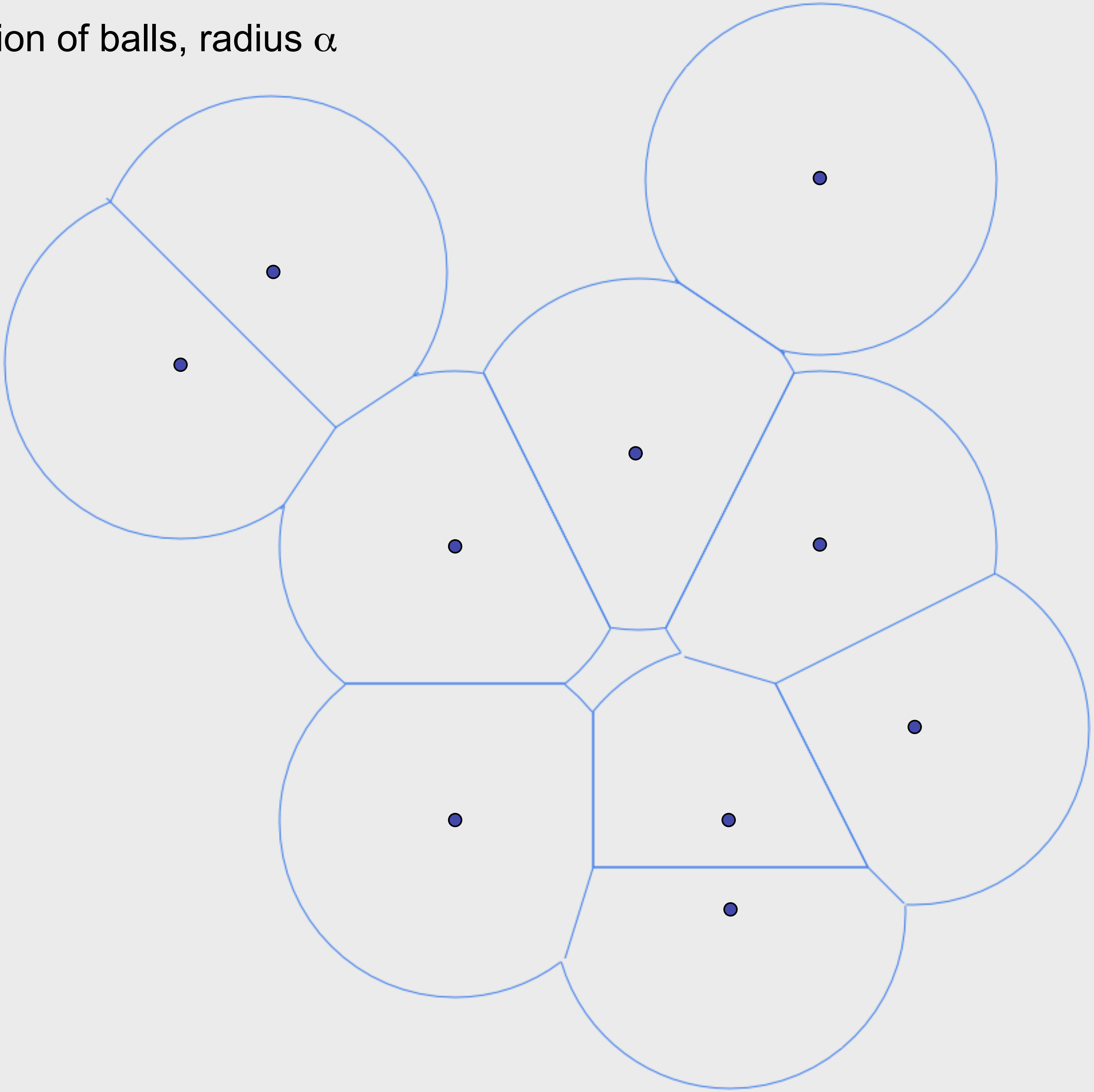

Alpha complex

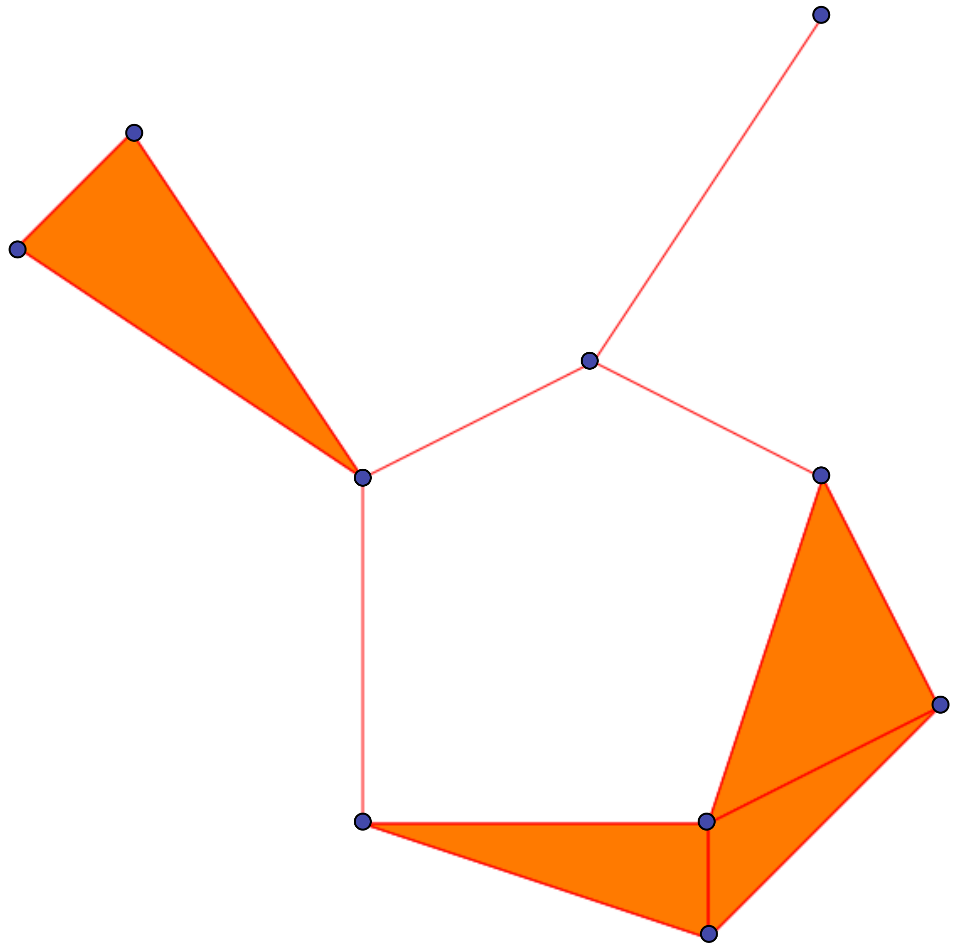

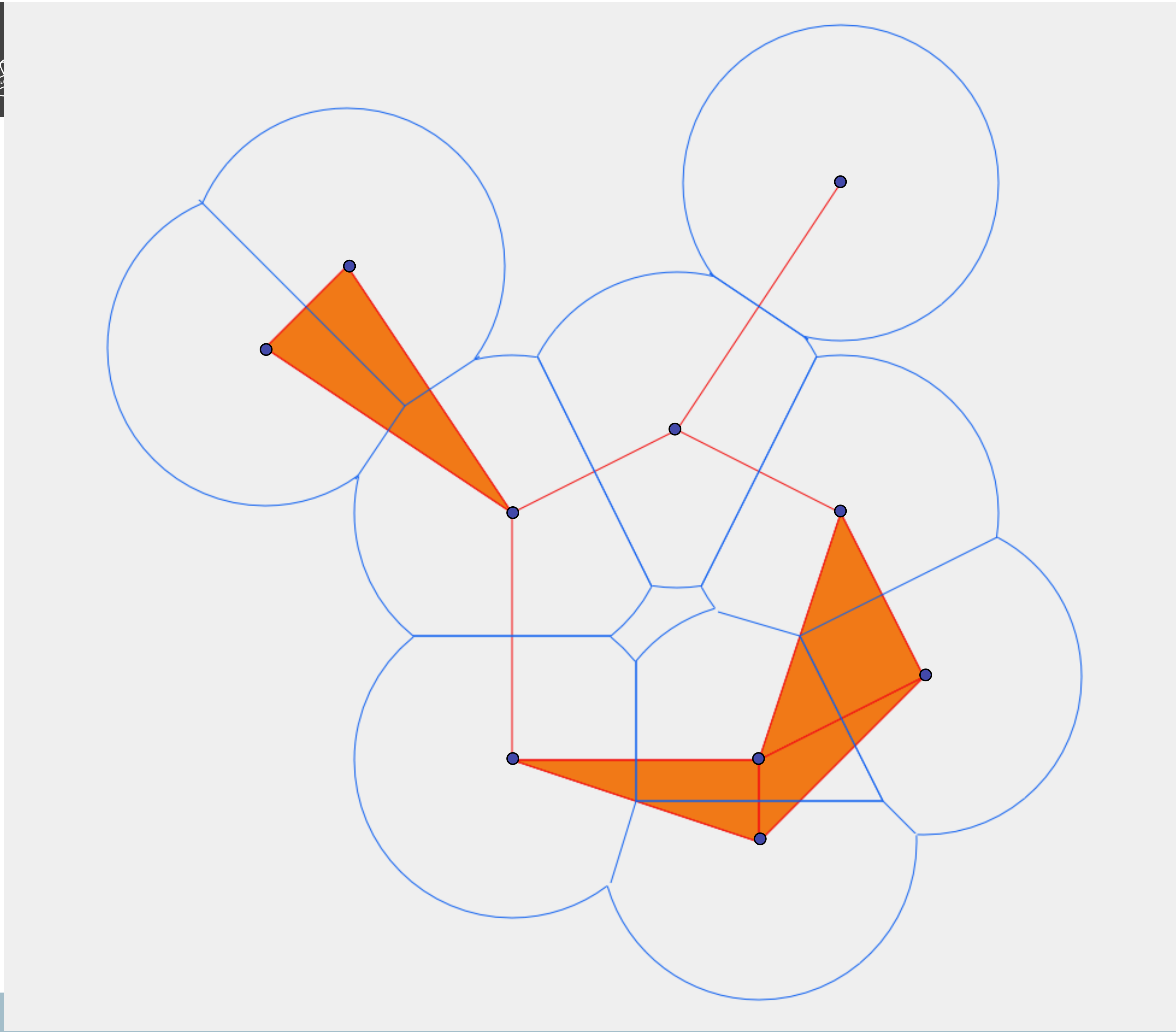

Alpha Shapes

Given a simplex, σ, in the Delaunay triangulation its alpha threshold, $\alpha_T(\sigma)$, is the radius of the smallest sphere that touches the vertices of σ and contains no other data points.

acute triangles

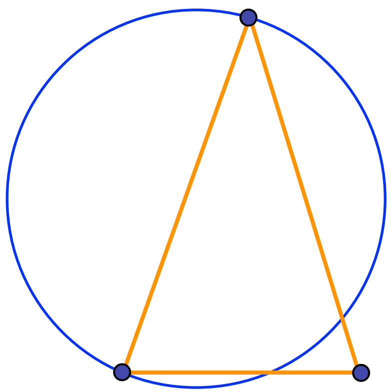

non-acute triangles

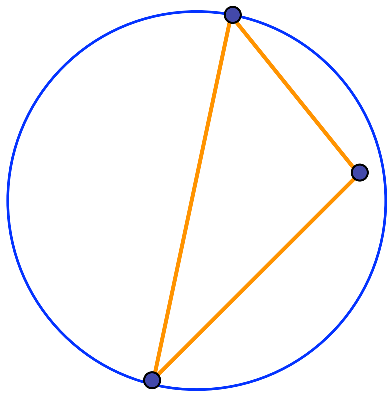

The alpha threshold of a lower dimensional face is not always the same as the circumradius of that face.

The alpha complex (or alpha shape) is the union of all σ from the Delaunay triangulation with $\alpha_T(\sigma) <= \alpha$.

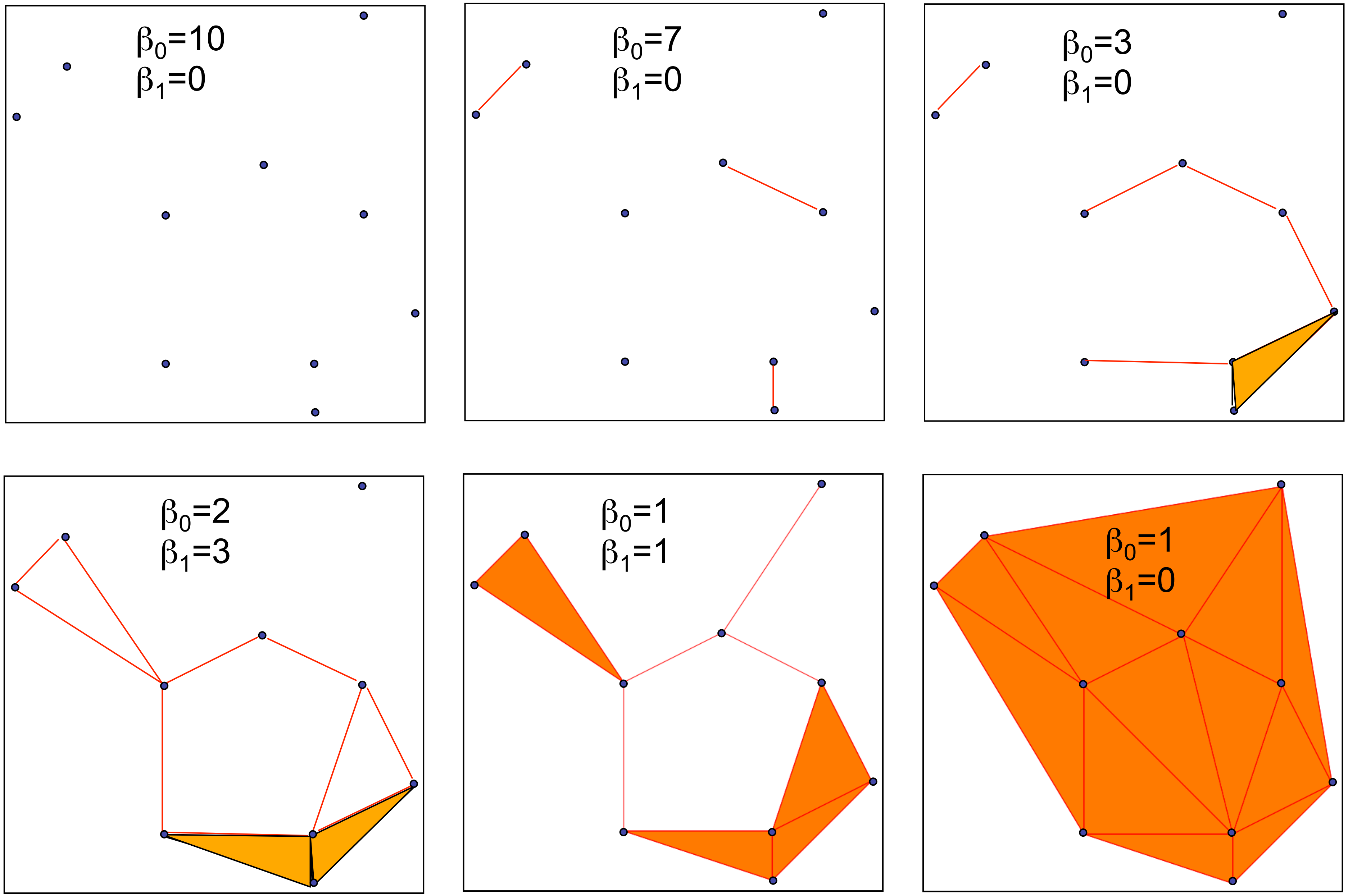

β_0=10
β_1=0
β_0=7
β_1=0
β_0=3
β_1=0
β_0=2
β_1=3
β_0=1
β_1=1
β_0=1
β_1=0

Incremental algorithm for BNs

- Add simplices one at a time.
- A k-simplex σ is positive if it creates a k-cycle; negative if it destroys a (k-1)-cycle.

- $\beta_k(\alpha)$ = #{+ve k-simplices with $\alpha_T <= \alpha$ }
  - #{-ve (k+1)-simplices with $\alpha_T <= \alpha$ }

- Algorithm due to Delfinado and Edelsbrunner (1993/5).
- Fast to compute in dimensions 2 and 3.

Homog. Poisson point patterns

- Computational model:
  - Constant intensity λ
  - N points in unit square with uniform distribution in each coordinate
  - For large λ, N is approximately Gaussian distributed.
  - Attach balls of radius α to each point.
  - Compute $\beta_k(\alpha)$ using periodic boundary conditions.
  - $E\beta_k(\alpha)$ estimated as mean values of many independent realizations in unit d-cube.

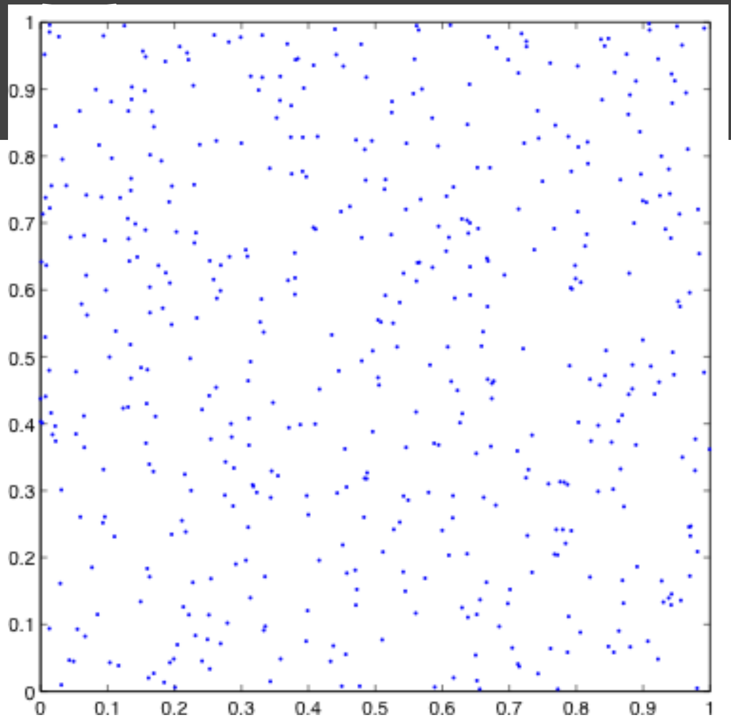

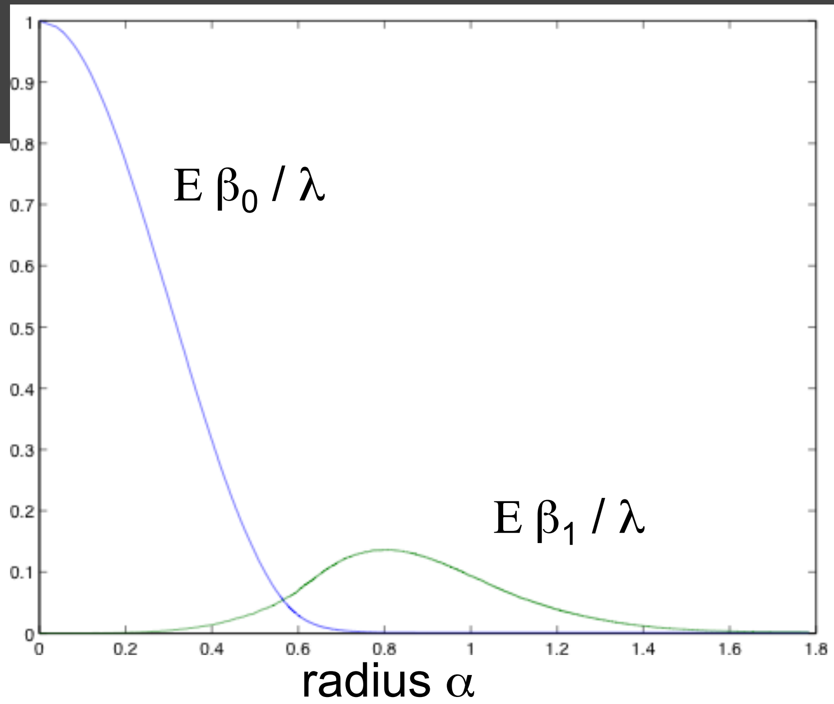

2D Asymptotic results:

$\beta_0 / \lambda = 1 - 2\eta + 1.5641\eta^2$

$\beta_1 / \lambda = 0.0640\eta^2$

η is $\pi\alpha^2\lambda$

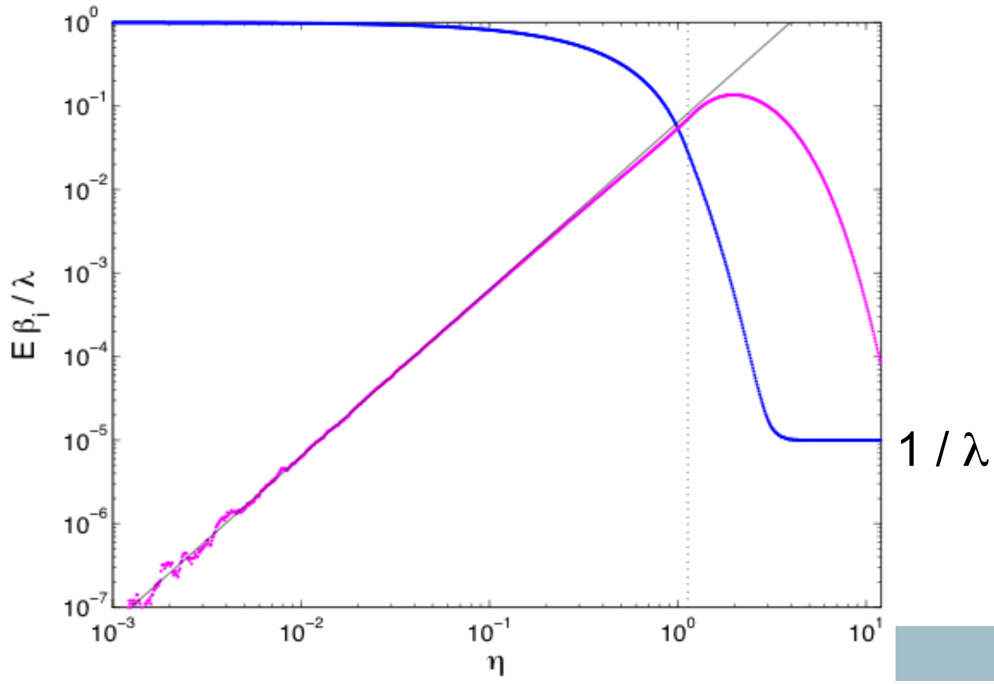

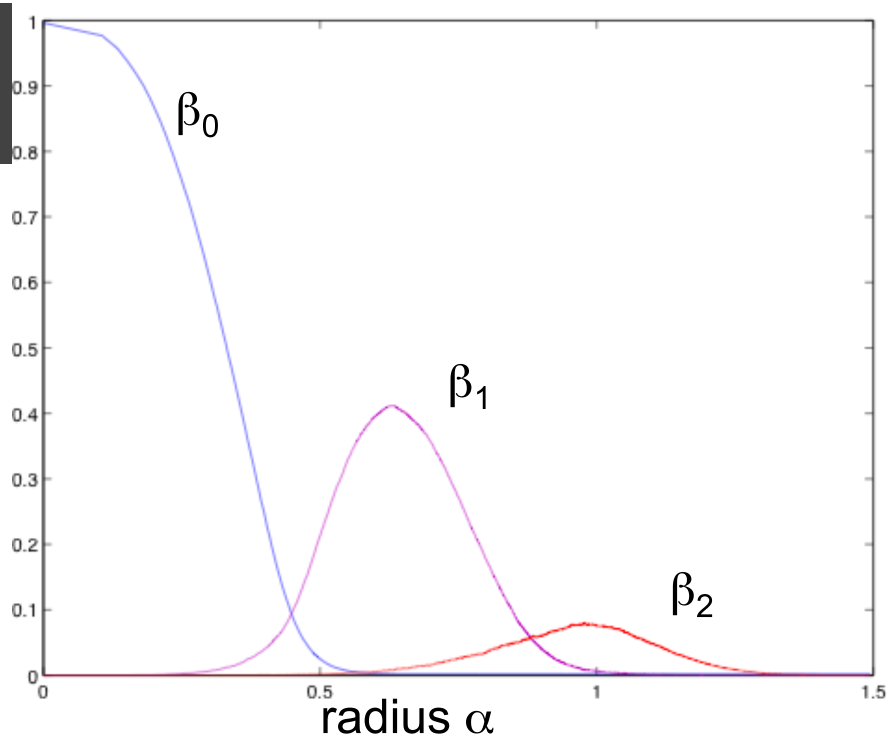

3D Asymptotic results:

$\beta_0 / \lambda = 1\text{-}4\eta+5\eta^2 -2.7431\eta^3$

$\beta_1 / \lambda = 0.5747\eta^2$

$\beta_2 / \lambda = 0.015\eta^3$

η is $(4/3)\pi\alpha^3\lambda$

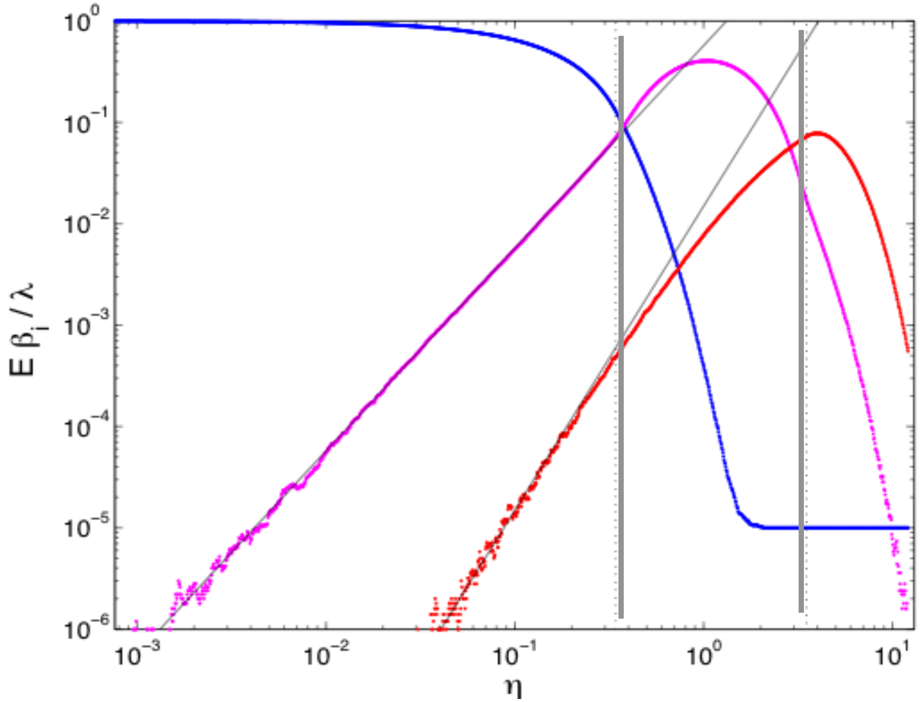

grey lines mark the direct and void percolation thresholds

Conjecture of Klaus Mecke that the zeros of the Euler function bound the percolation thresholds.
See Naher et al J Stat Mech 2008

Australian National University

Derivation of results

- Results for β_0 are due to Quintanilla and Torquato, 1996.
- For β_1 we use the following result due to Miles (1974)
- Size and shape of a Poisson Delaunay cell is completely characterised by the p.d.f.

$$h_m(r,\mathbf{u}_0,\ldots,\mathbf{u}_m) = a(\lambda,m)\Delta_m r^{m^2-1}\exp(-\lambda\omega_m r^m).$$

- Ergodicity of the Poisson-Delaunay complex implies

  E #{σ in R such that σ is A} = λ_k ||R|| Pr(A)

Empty triangles in 2D

- Simplest hole in 2D alpha shape is formed by edges of a single triangle

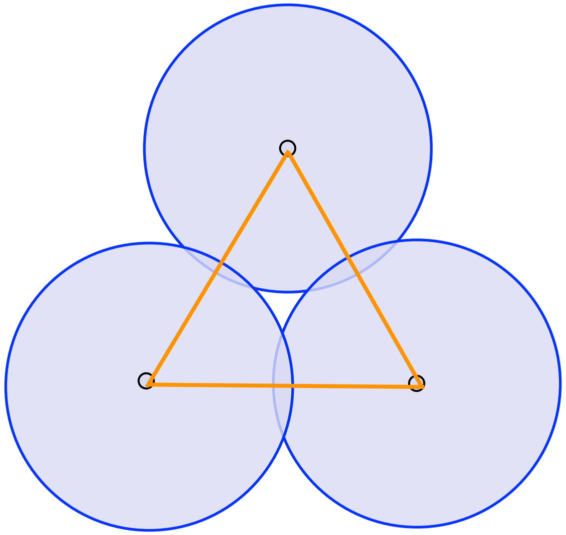

Property A is:

- All edges < 2α
- Triang. circumradius > α
- Acute triangle

$$P_{\Delta} = \int_{\pi/3}^{\pi/2} \int_{\alpha}^{\alpha/\sin\phi} 2(\pi\lambda)^2 r^3 e^{-\pi\lambda r^2} f_{\max}(\phi)\, dr\, d\phi.$$

$E\beta_1(\alpha) >= 2\lambda \Pr(A) \sim 0.0640\, \lambda\, \eta^2$

Higher order terms

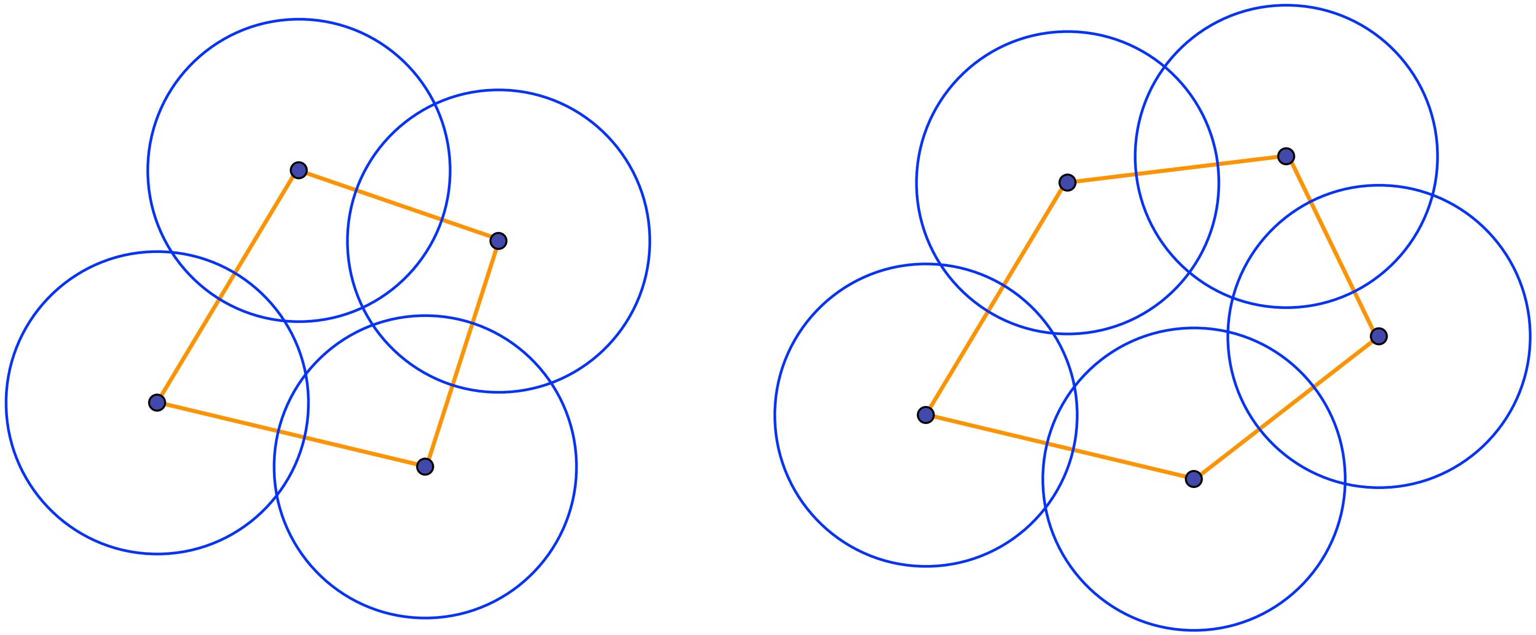

…Need joint distributions of two or more PDC triangles.

Or some clever tricks analogous to Torquato's expressions for the number of clusters containing k spheres

Empty triangles and tetrahedra

- Similar argument as in 2D case.

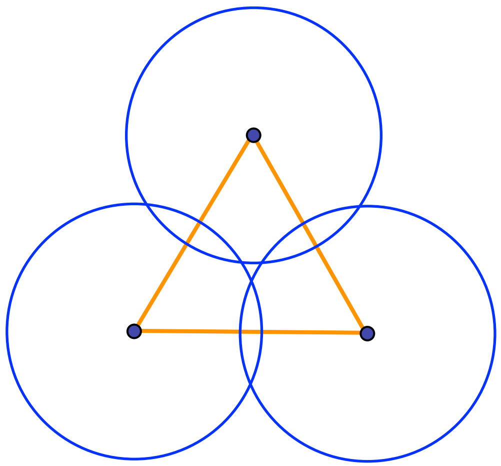

Triangle conditions now
apply to a typical face of a PDC

$E\beta_1(\alpha) \sim \lambda_2 \, \Pr(A) \sim 0.5747 \, \lambda \, \eta^2$

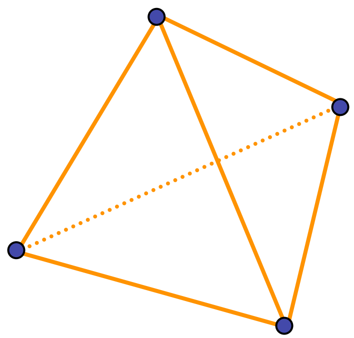

Face circumradii < a
Tetrahedron circumradius > a
Circumcenter interior to tetrahedron.

$E\beta_2(\alpha) \sim \lambda_3 \, \Pr(A) \sim 0.015 \, \lambda \, \eta^3$

Persistent homology

X_a maps inside X_b

So there is a linear map

$\pi: H_k(X_a) \longrightarrow H_k(X_b)$

define $H_k(a,b)$ to be

$\pi(H_k(X_a)) \subset H_k(X_b)$

$H_k(a,b)$ encodes cycles in X_a equivalent wrt boundaries in X_b

Persistent homology is defined for a growing sequence of cell complexes

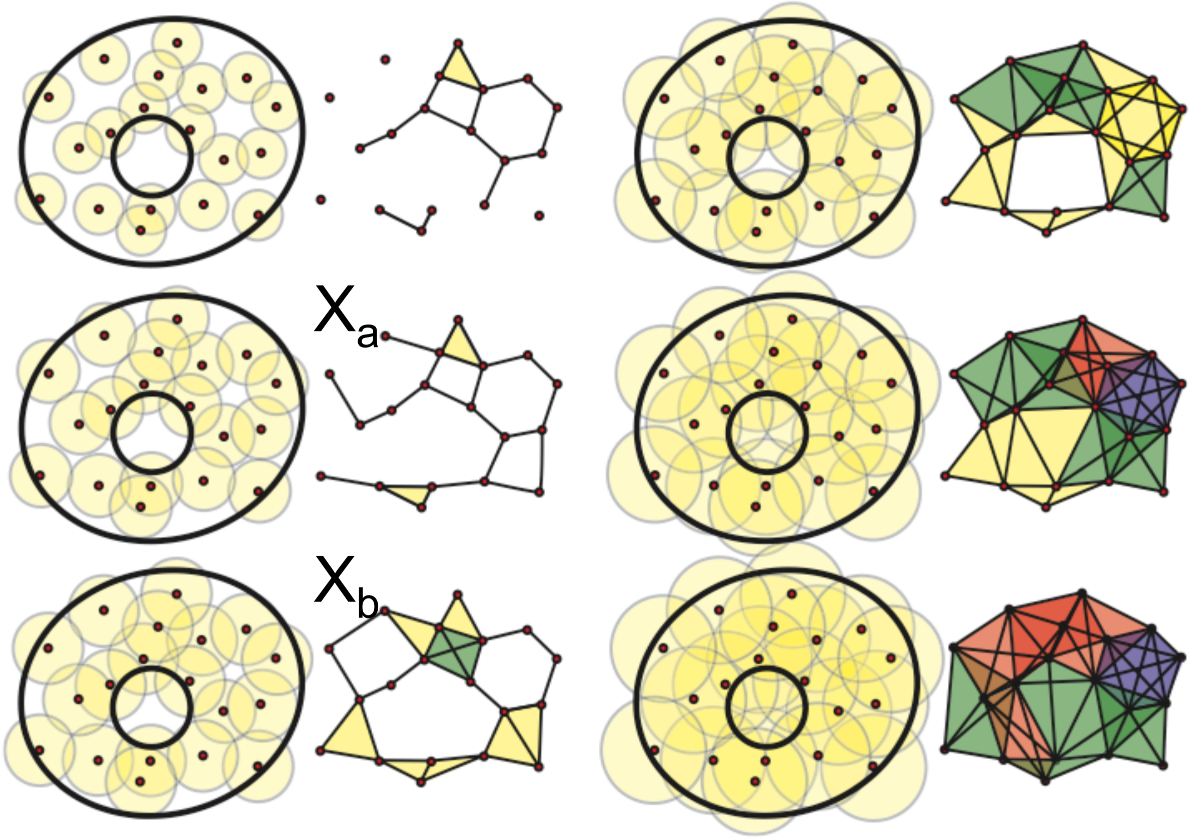

Robins (1999) “Towards computing homology from finite approximations”
Edelsbrunner, Letscher, Zomorodian (2000) “Topological persistence and simplification”
Zomorodian, Carlsson (2005) “Computing persistent homology”

image from Ghrist. Barcodes: the persistent topology of data. Bulletin AMS 2008

Australian National University

Persistent homology

- Input: A filtration: $K_0 \subset K_1 \subset K_2 \subset \cdots \subset K_n$
- i.e. an ordering of the cells in the complex.

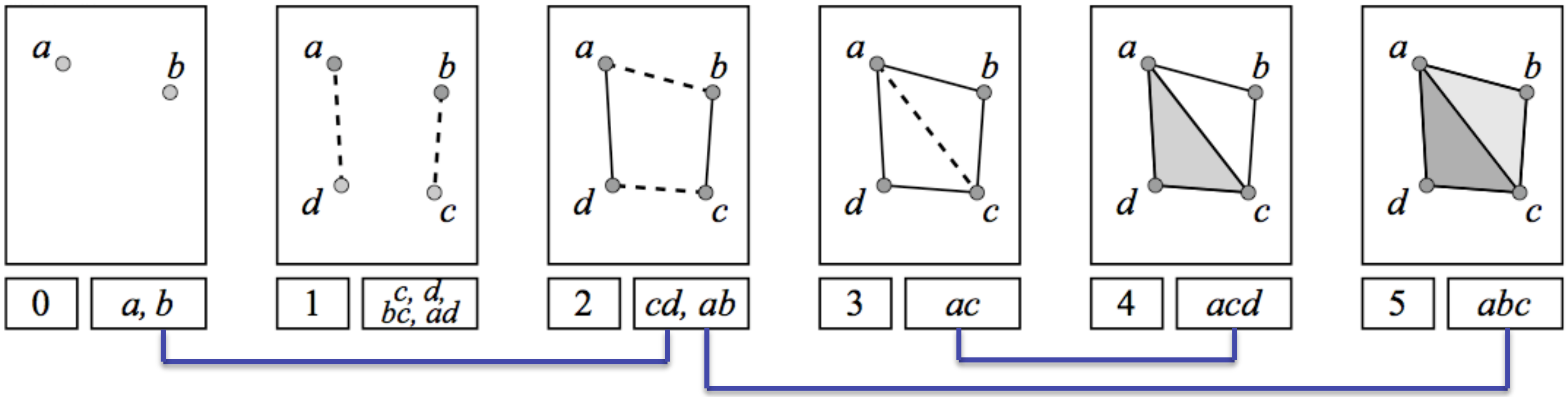

- cells are added sequentially (never removed).
- each *k*-cell either creates a *k*-cycle or destroys a *(k-1)*-cycle.
- a destroyer is paired with the youngest cycle that is homologous to its boundary.
- Output: (birth, death) pairs that define the parameter interval over which each *k*-cycle exists.

image from Zomorodian (2009) Computational Topology

Persistence diagrams

persistence barcode

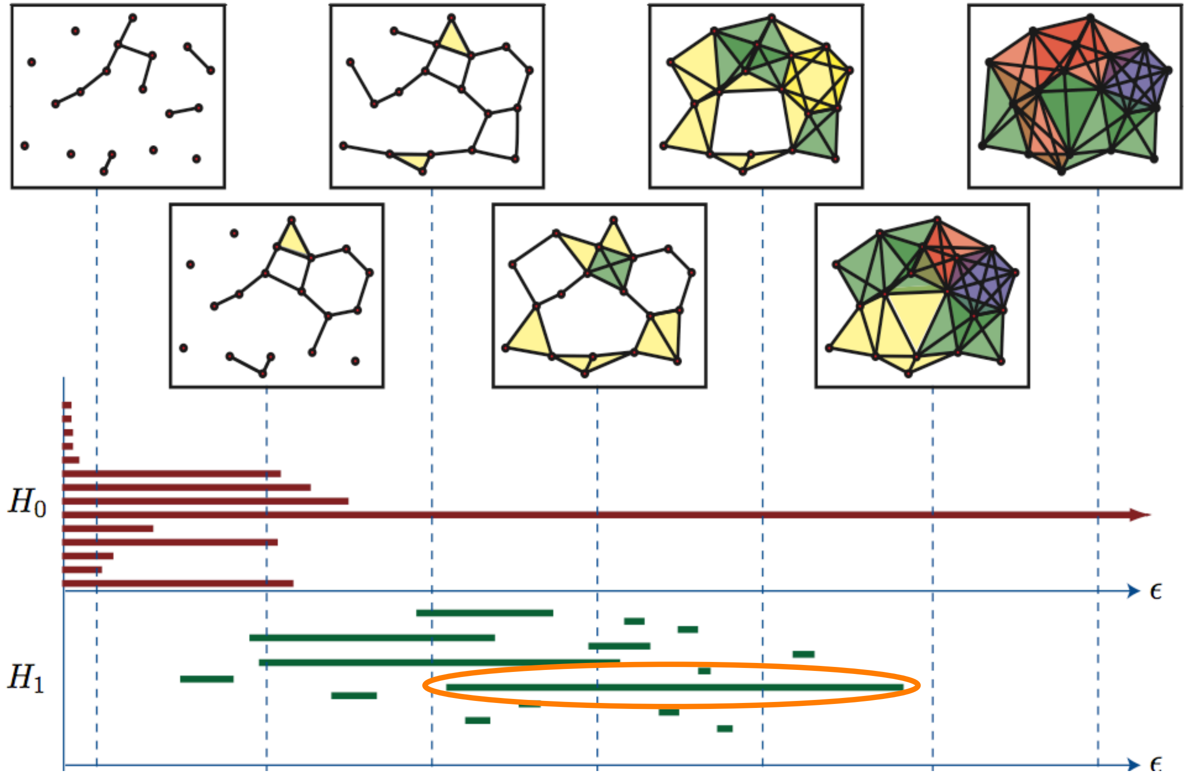

persistence diagram

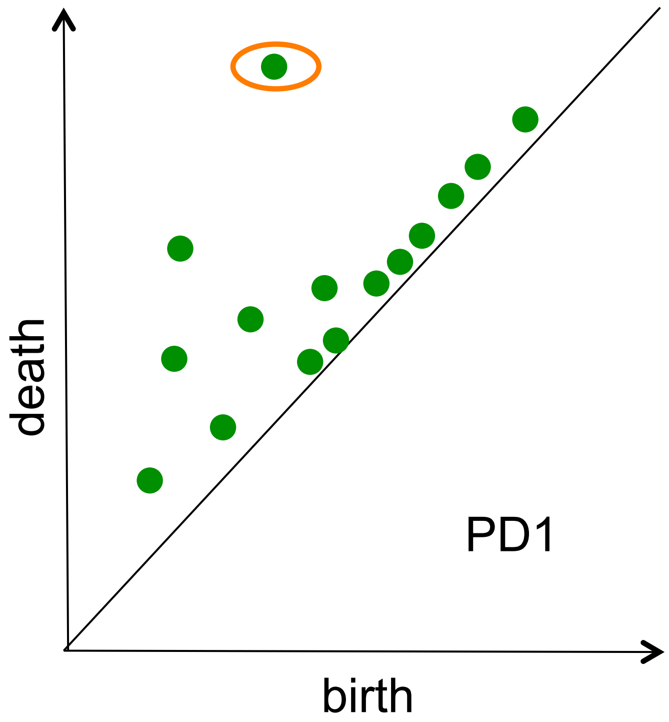

Key result: Persistence diagrams are stable wrt to perturbations in the original data [Cohen-Steiner, Edelsbrunner, Harer (2007) "Stability of persistence diagrams"]

image from Ghrist. Barcodes: the persistent topology of data. Bulletin AMS 2008

spherical bead packing

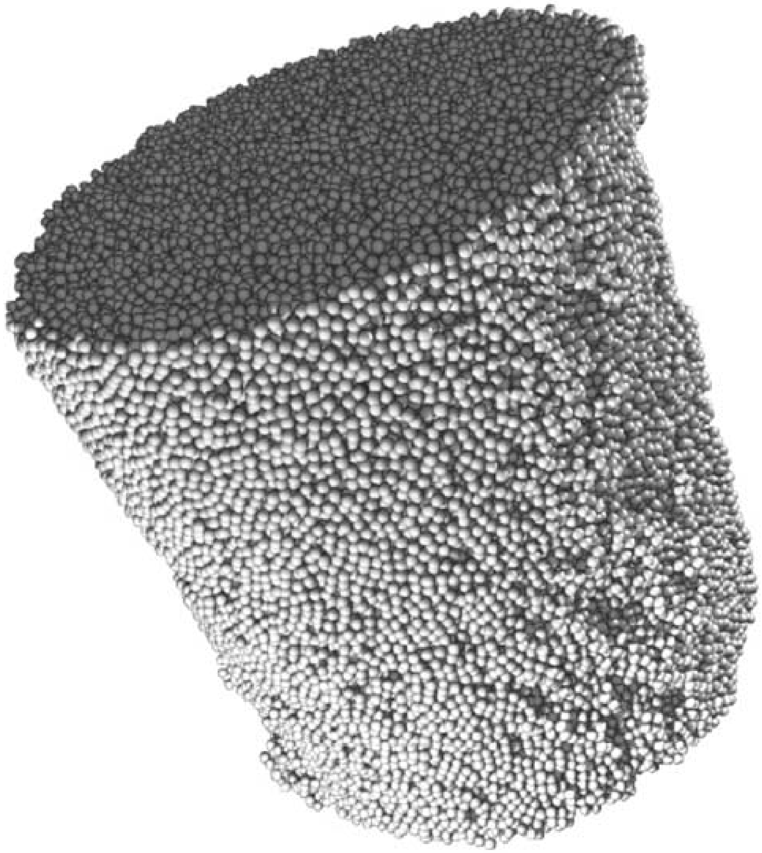

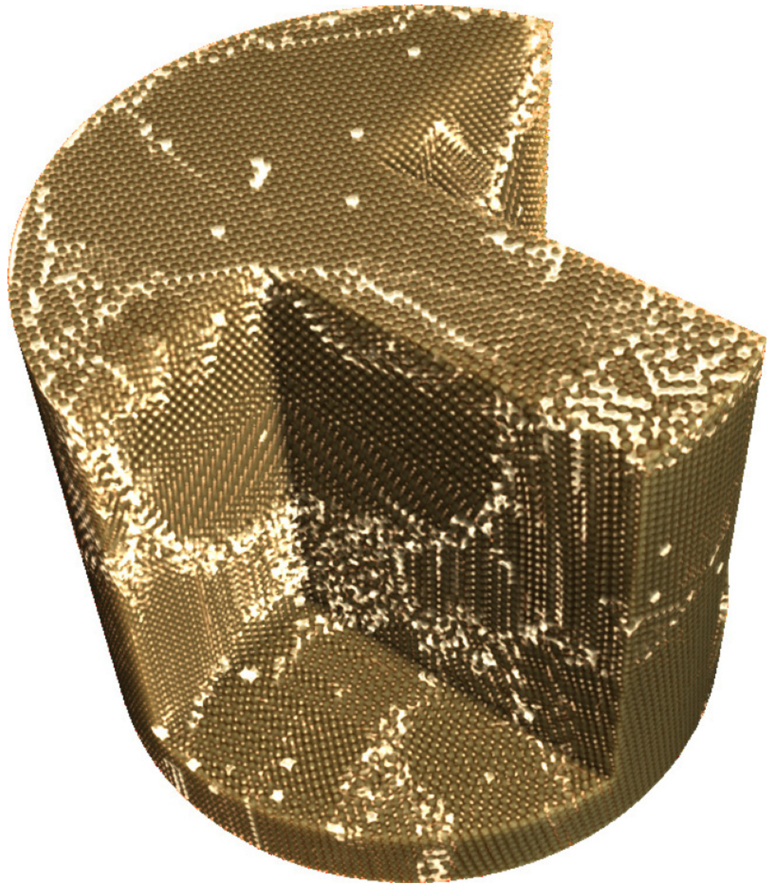

Disordered packing
(random close pack, maximally jammed)
Bernal limit has vol frac Φ = 64%
Well-defined distribution of local volumes

Partially crystallized packing, Φ=70%
a fully crystallized packing has Φ=74%
Kepler's conjecture (1600s) has only been proven this century by Hales and Ferguson

spherical bead packing

Data analysis:

1. calculate bead centres and radii from the XCT image
2. build the Delaunay complex from the bead centres
3. construct the alpha-shape filtration
4. compute persistence diagrams

2-4 use CGAL and dionysus software packages.

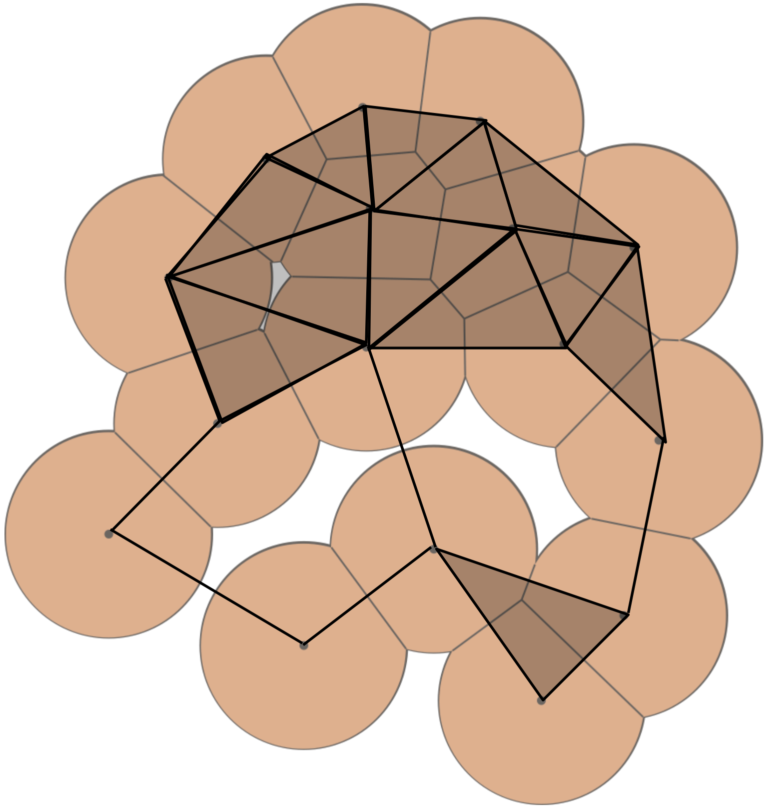

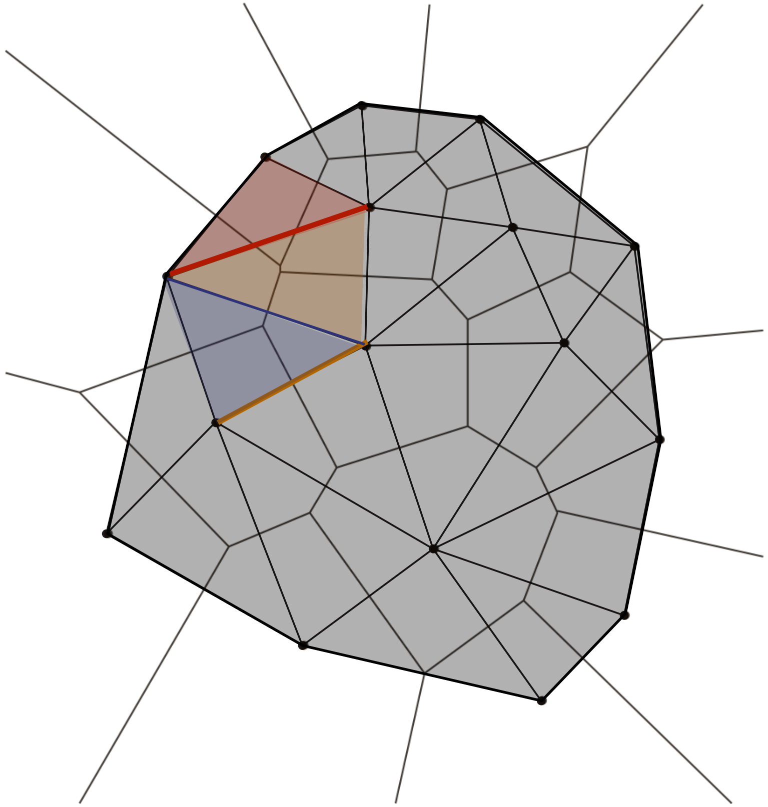

spherical bead packing

A maximally dense packing is built from layers of hexagonally packed spheres
Locally, these give pores related to regular tetrahedra and octahedra

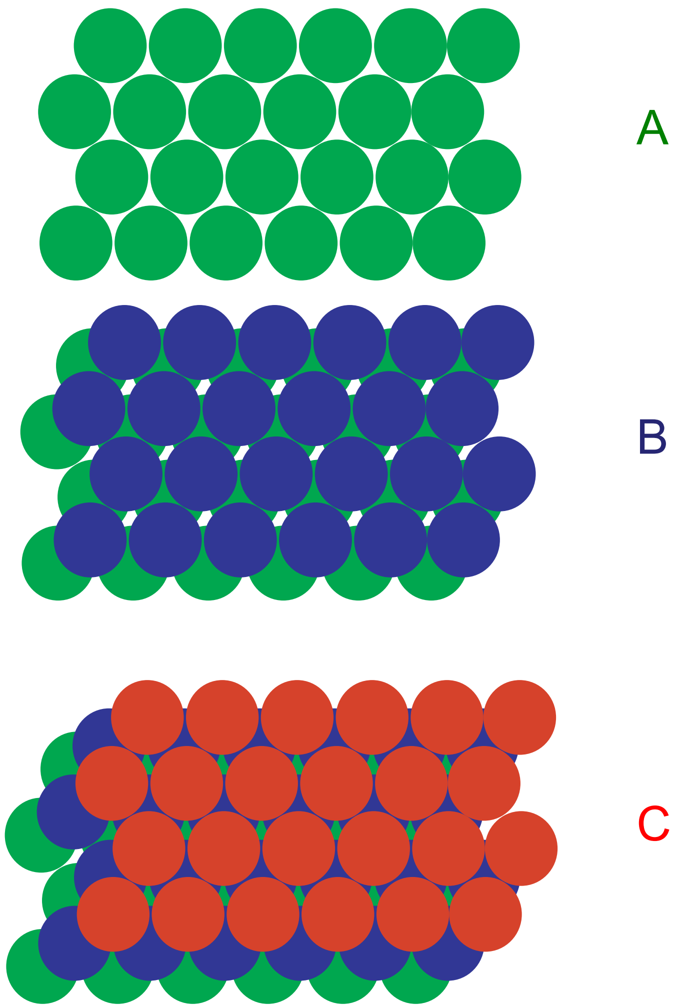

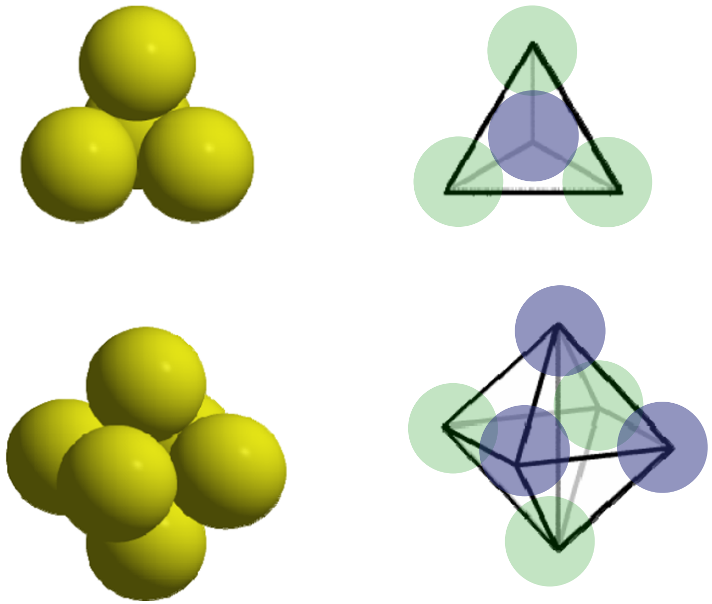

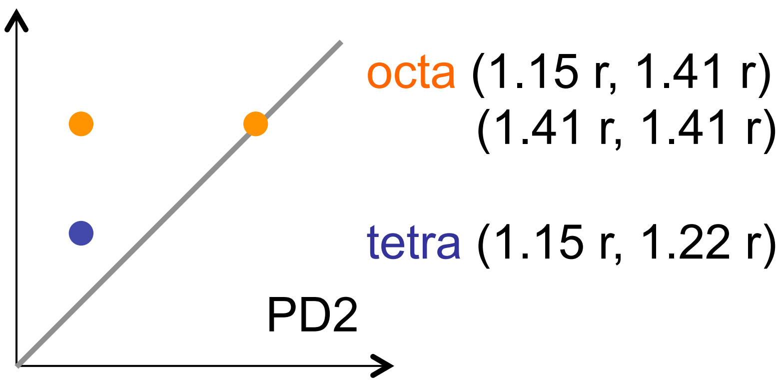

spherical bead packing

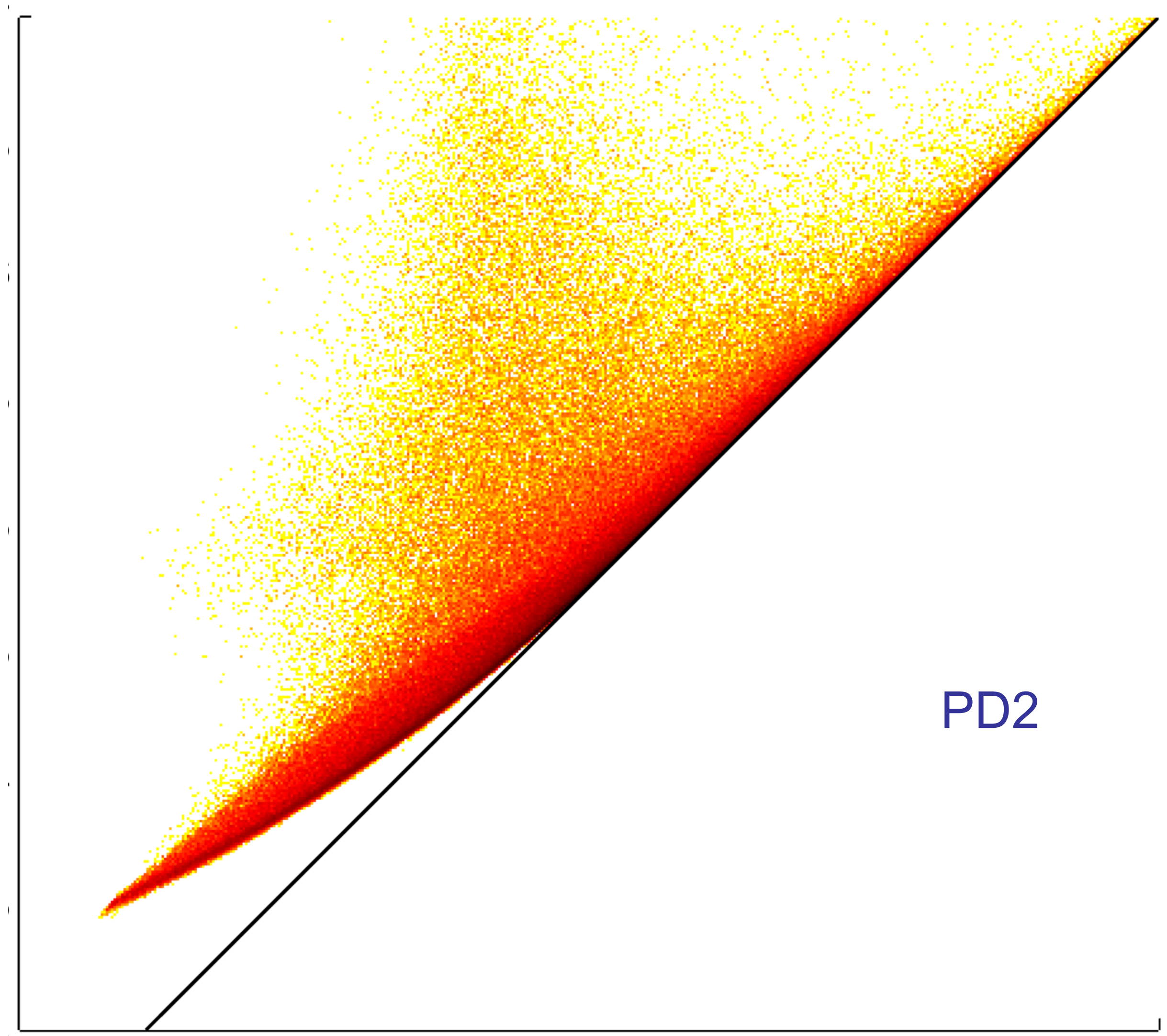

packing fraction
0.59

PD2

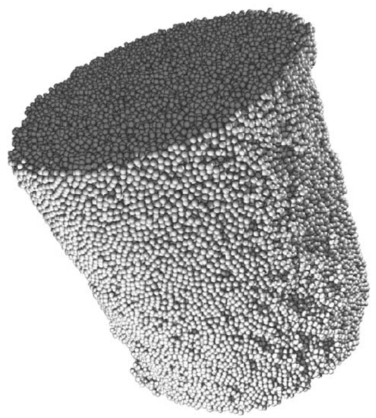

spherical bead packing

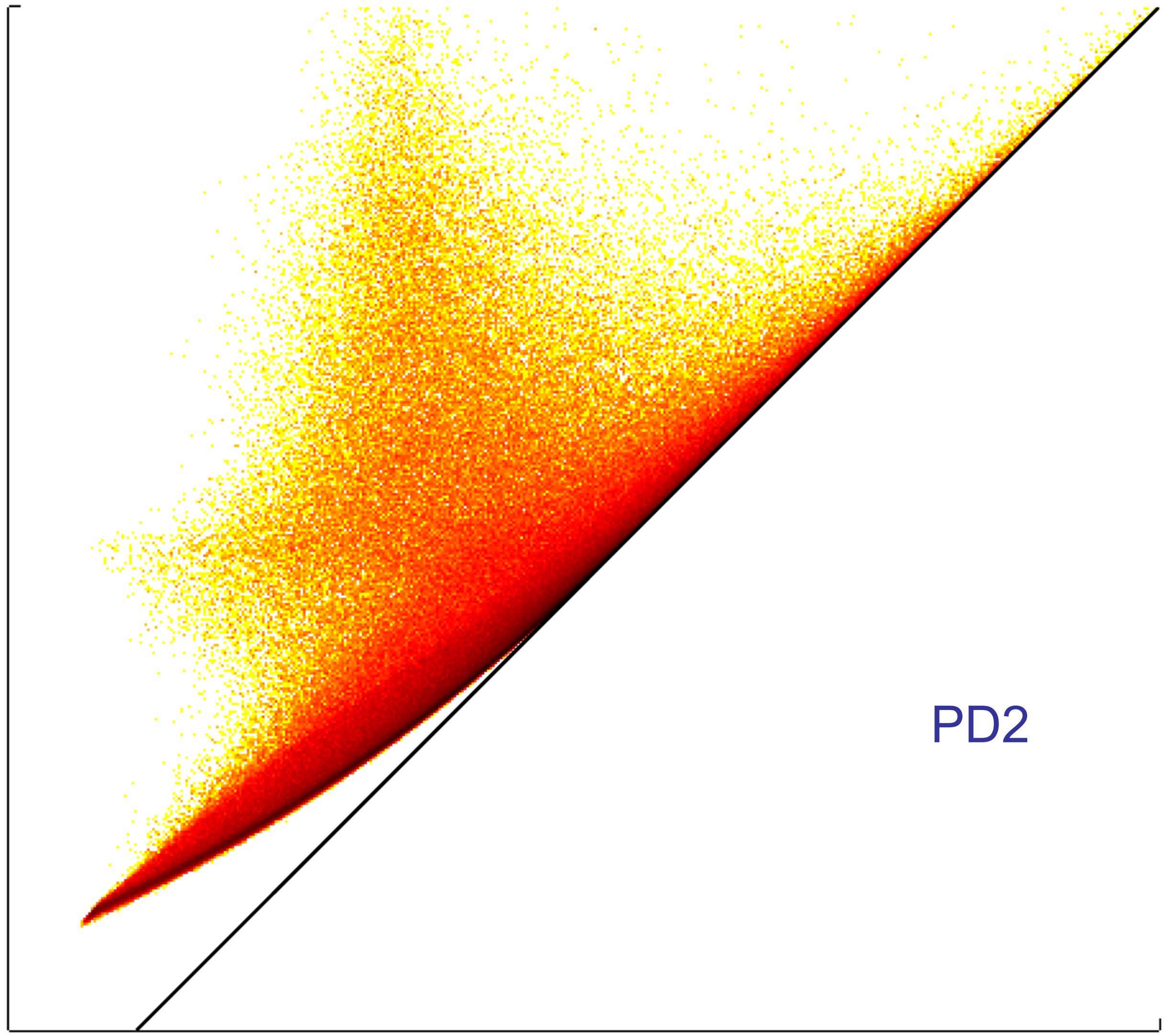

packing fraction
0.63

PD2

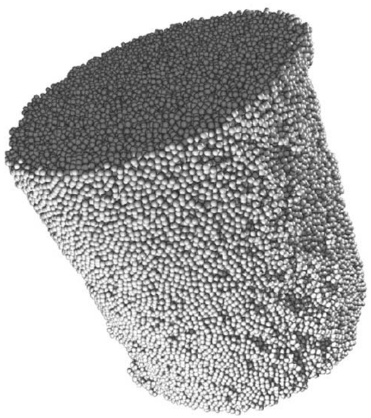

spherical bead packing

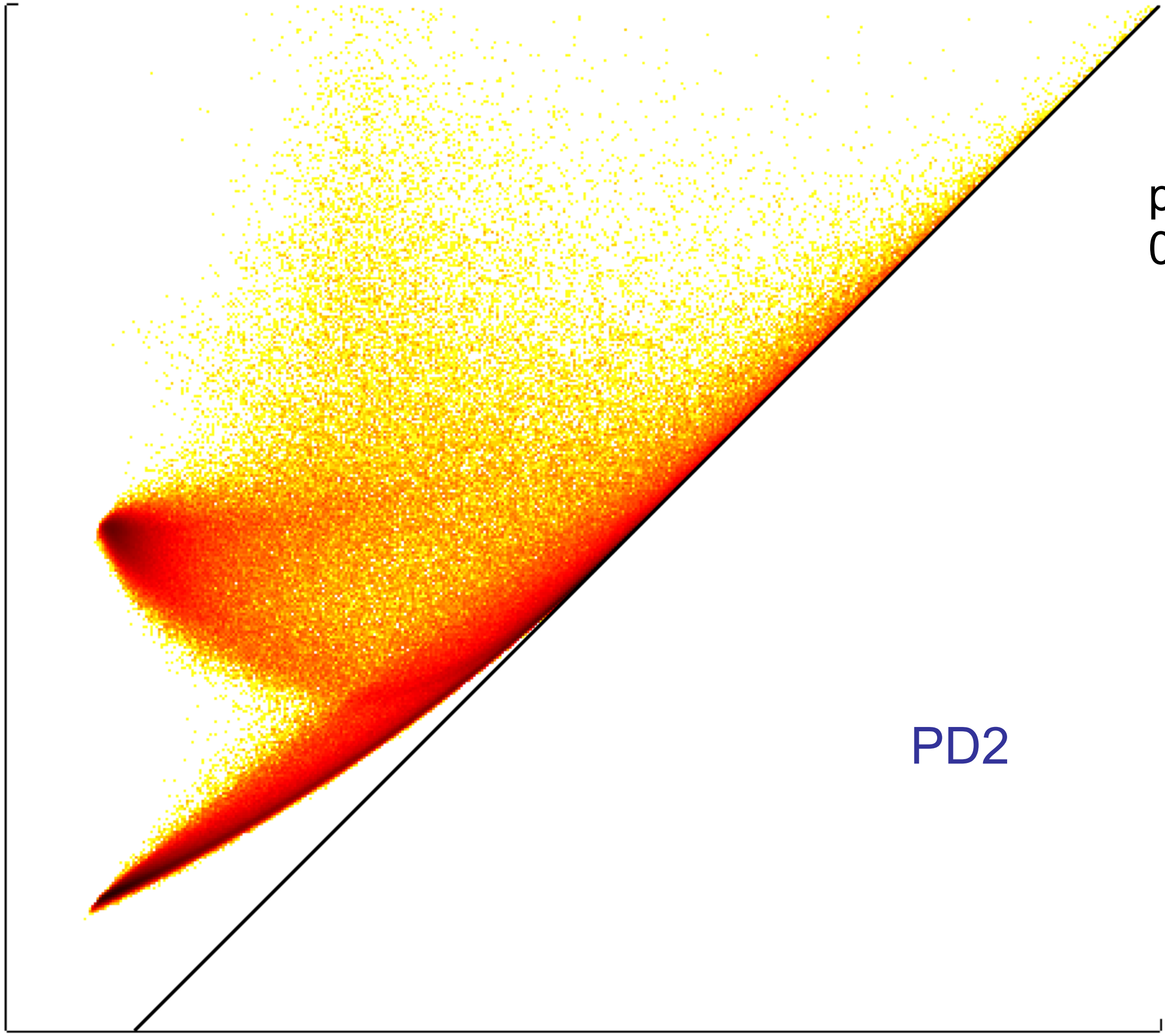

packing fraction
0.70

PD2

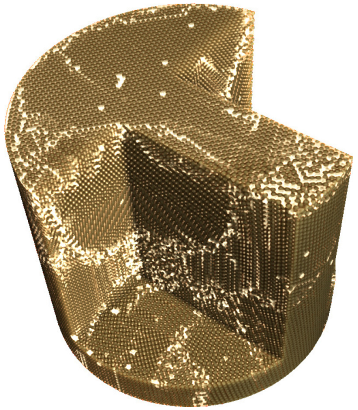

spherical bead packing

Saadatfar, Takeuchi, Robins, Francois, Hiraoka (2016) in review.

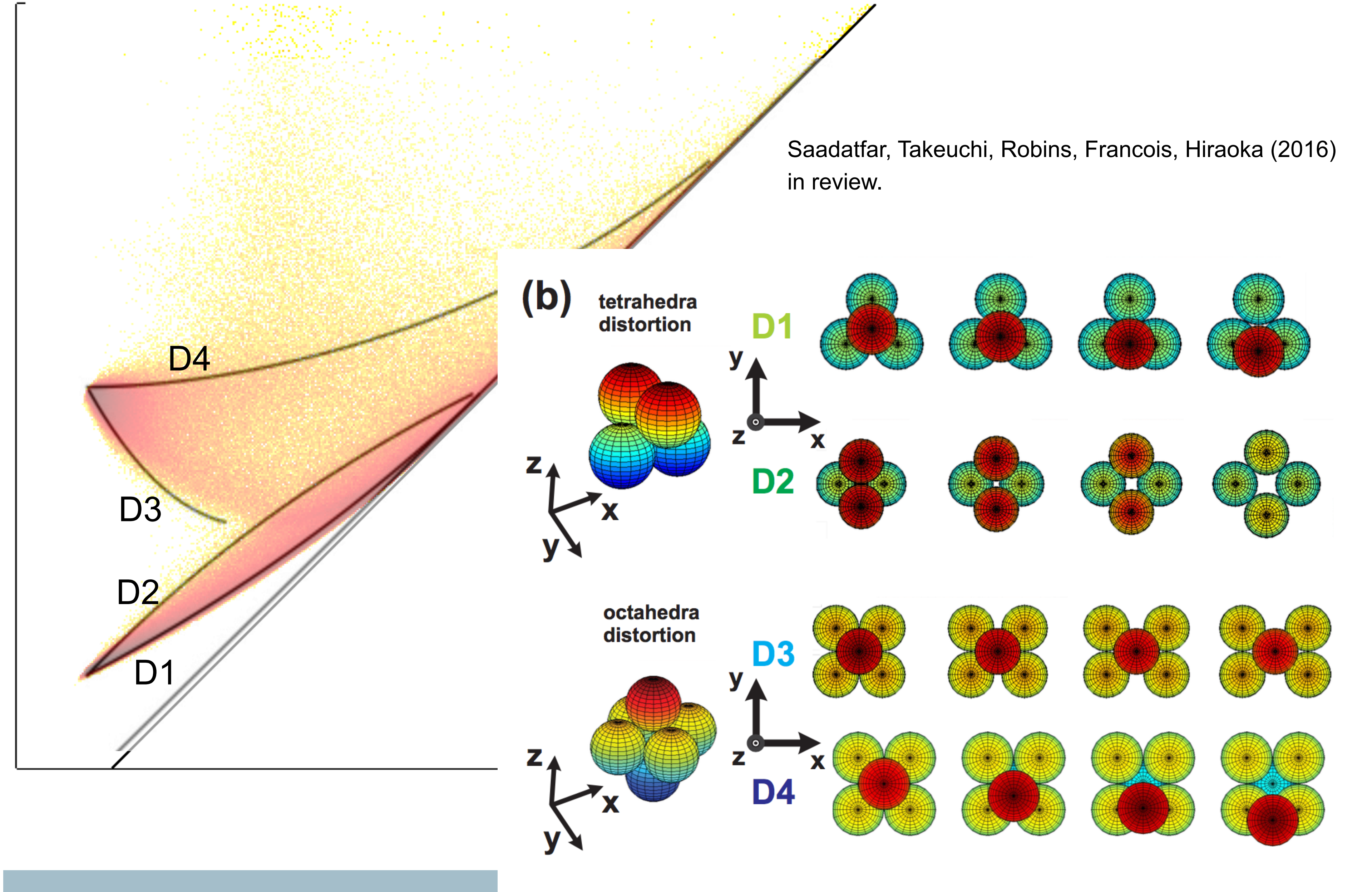

spherical bead packing

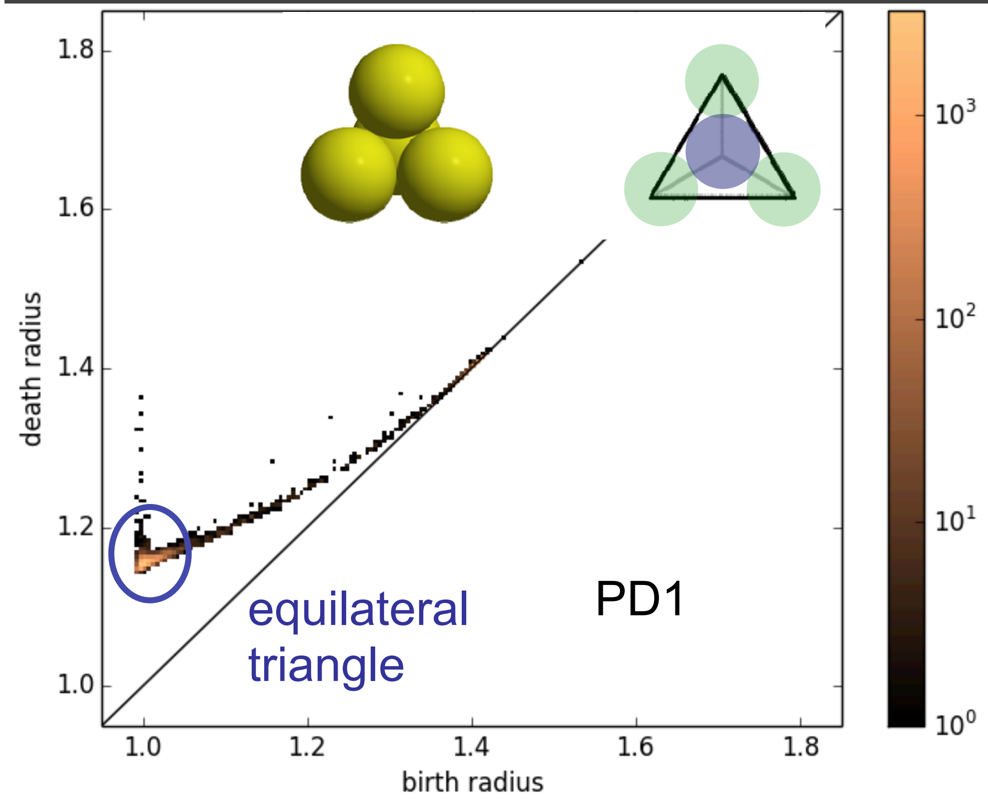

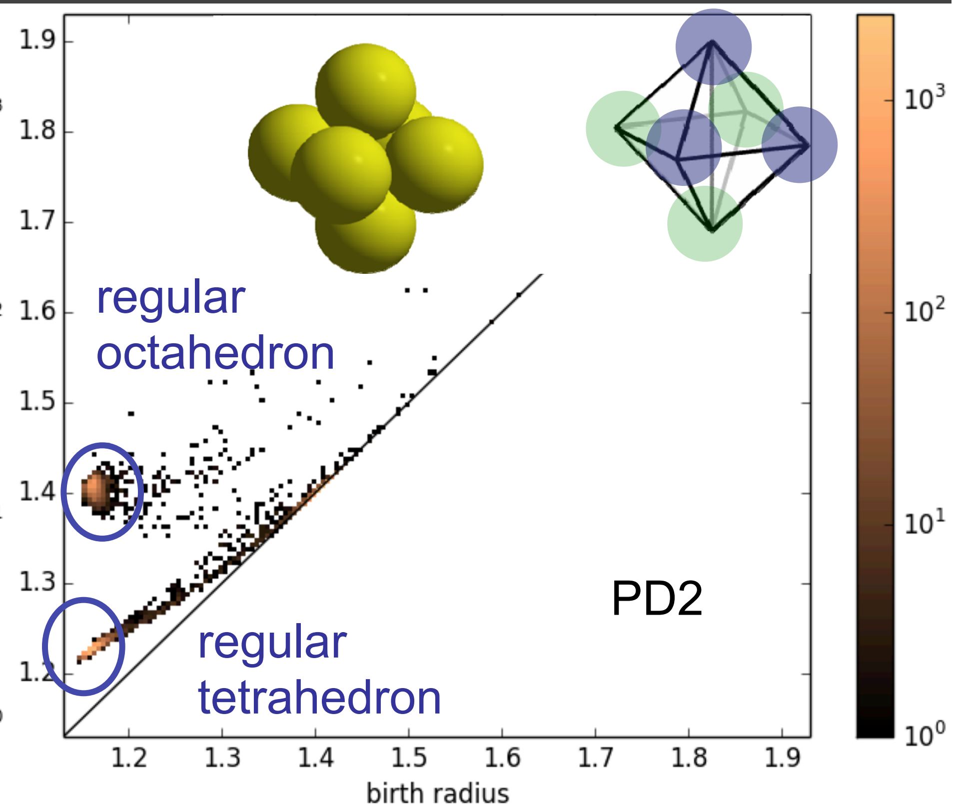

Persistence diagrams for a subset (14mm^3) of the partially crystallised packing with high volume fraction = 72%.

axis units normalised by bead radius = 0.5mm

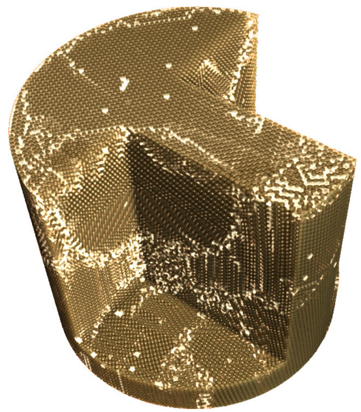

spherical bead packing

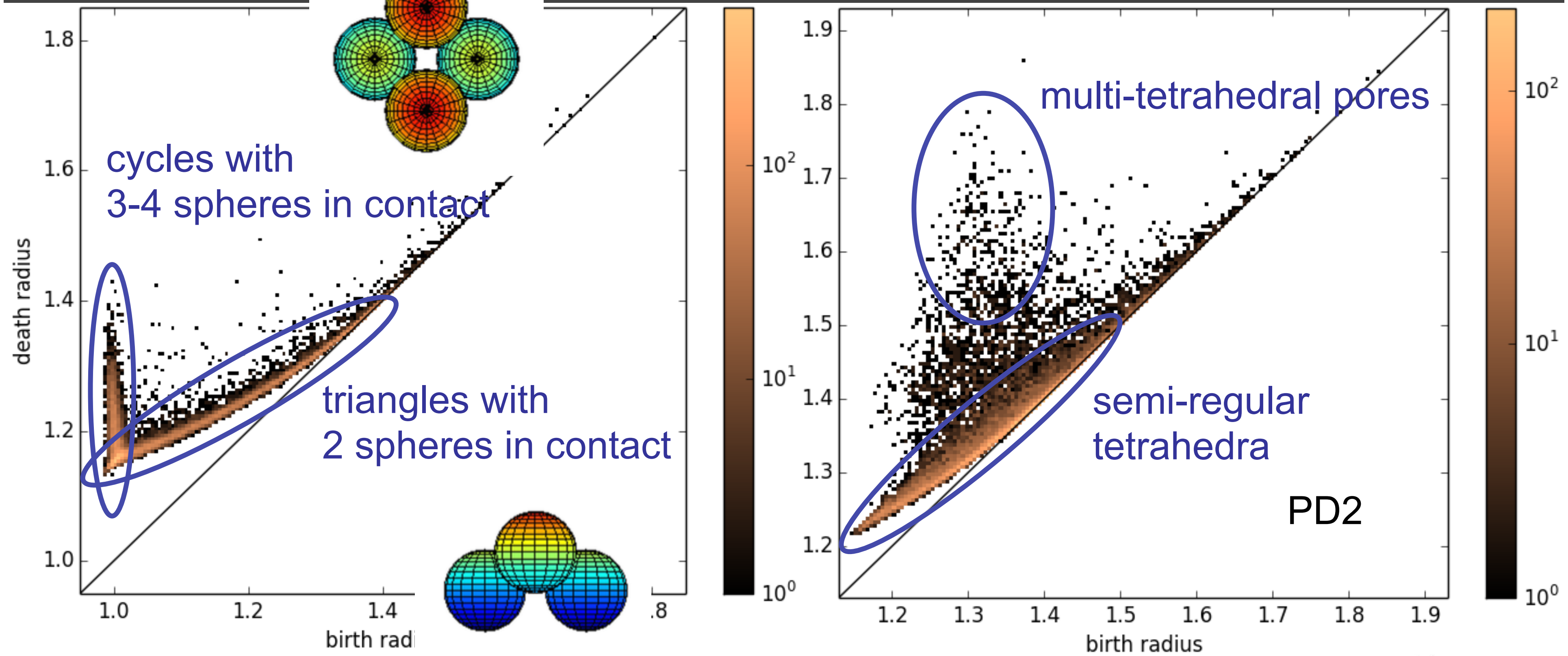

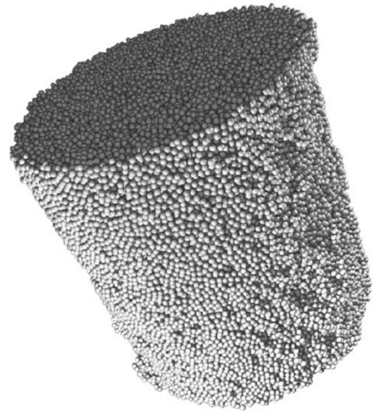

Persistence diagrams for a subset (14mm^3) of the random close packing with volume fraction = 63%.

the plots are 2D histograms where colour is log10 of the number of (b,d) points in a small box

axis units normalised by bead radius = 0.5mm

regular tet and oct pores

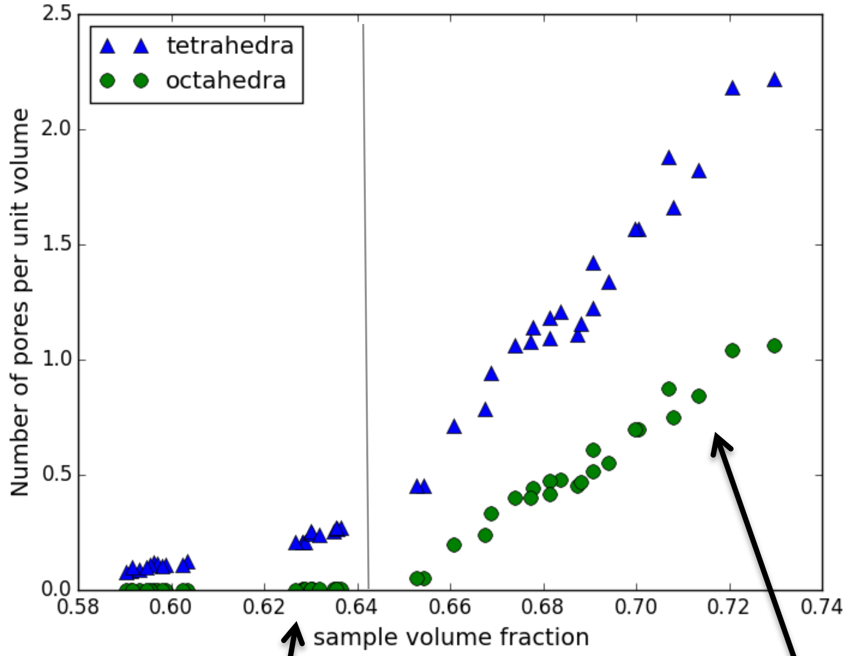

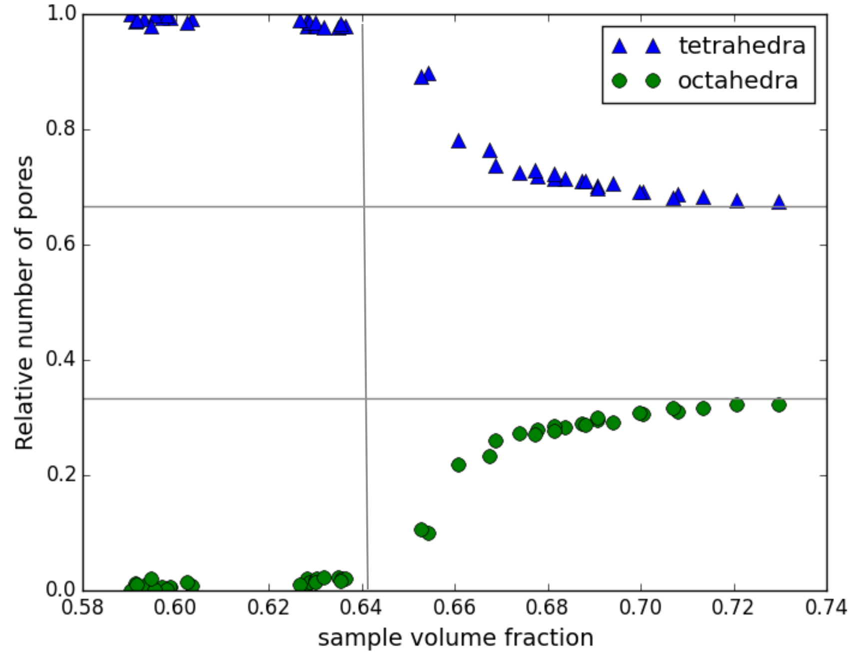

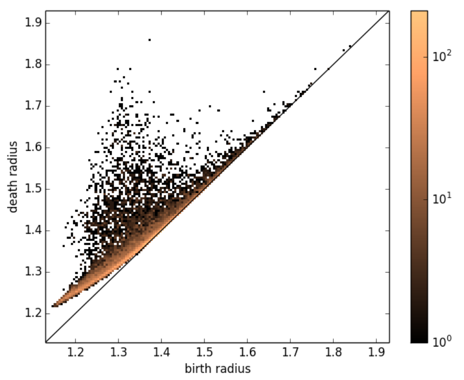

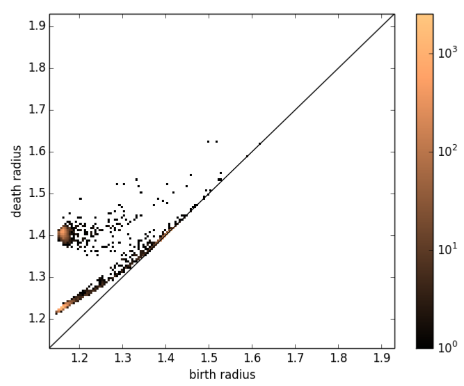

Notice the second transition at 67-68%

functional PCA of persistence diagrams from 36 subsets shows 97% of variation in their PD2 is explained by a single dimension

VR, Turner (2016) Physica D.

granular and porous materials

1mm scale bars

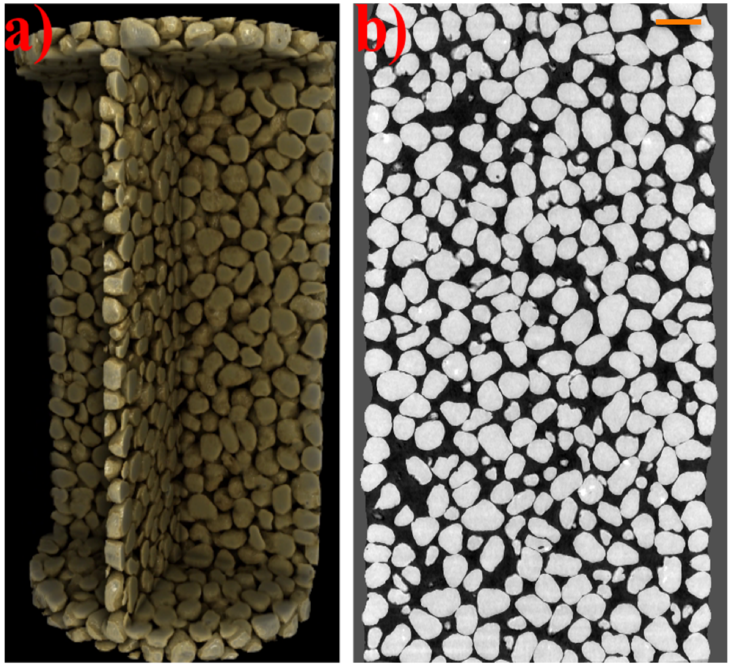

Ottawa sand

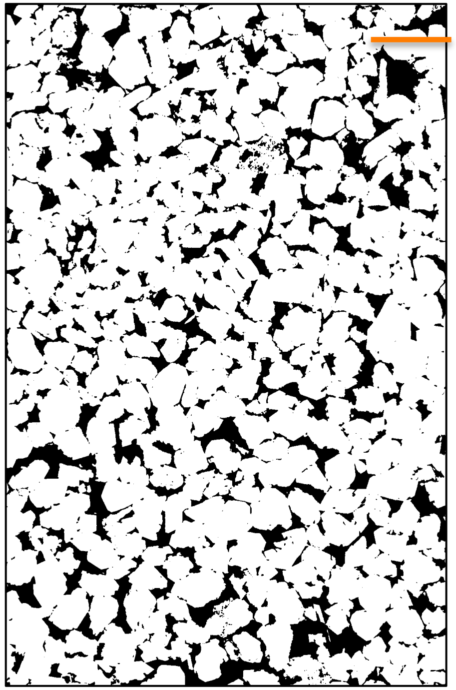

Clashach sandstone

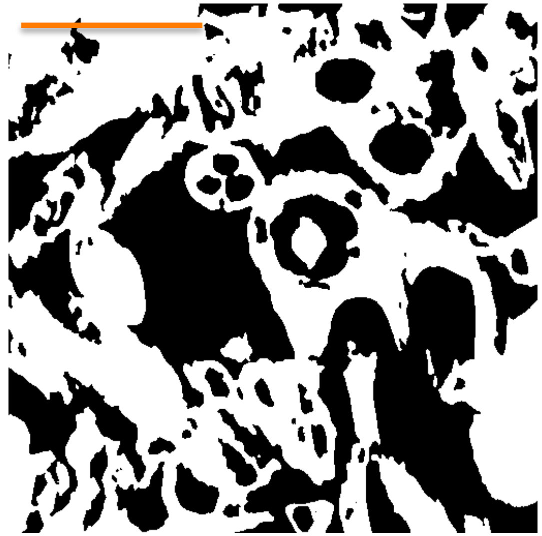

Mt Gambier limestone

Want accurate geometric and topological characterisation from x-ray micro-CT images

- pore and grain size distributions, structure of immiscible fluid distributions
- adjacencies between elements, network models

Understand how these quantities correlate with physical properties such as

- diffusion, permeability, mechanical response.

Topological image analysis

- Segment XCT image into grain (white) and pore (black) regions.
- Compute the signed Euclidean distance transform:
  - SEDT(x) = - dist(x, B) if x is in W
  - SEDT(x) = dist(x,W) if x is in B

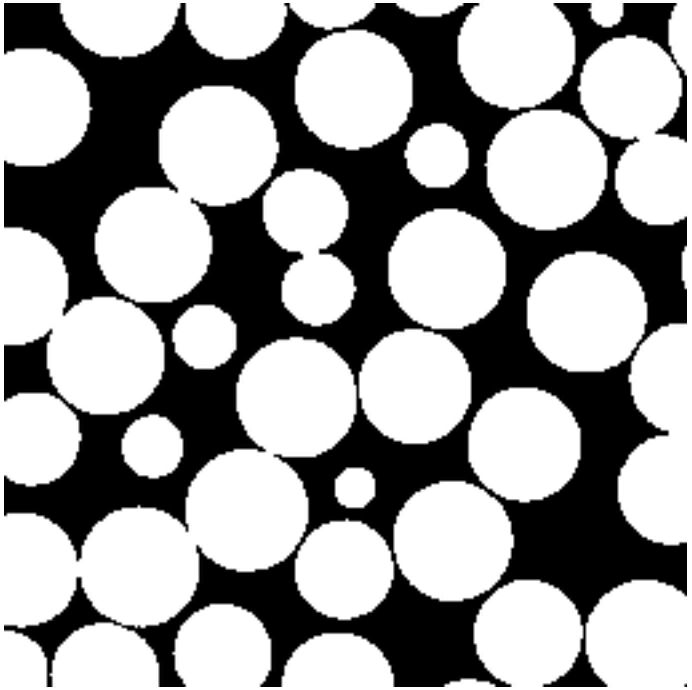

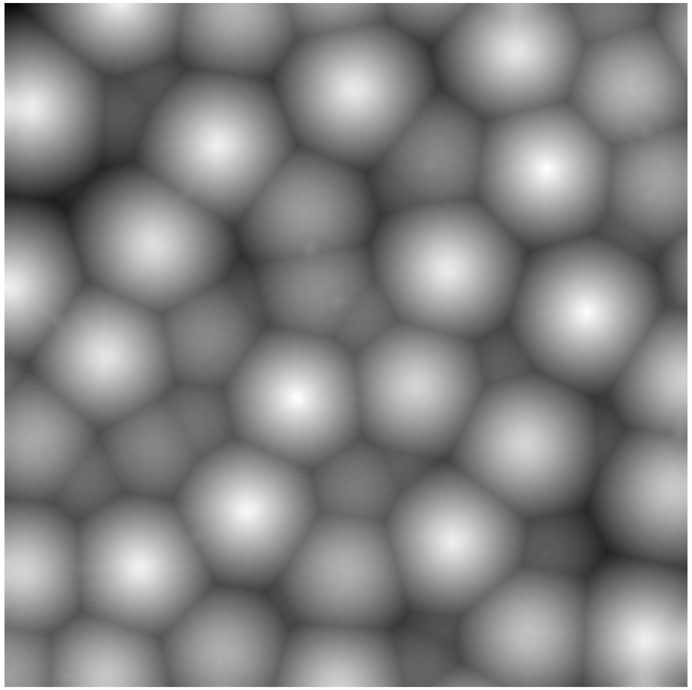

Topology from images

What is the filtration for persistence?

Imagine grey levels are heights in a landscape, study the lower level sets: $f(\mathbf{x}) \leq h$.
The topology can only change when h passes through a critical value.

This observation goes back to JC Maxwell and was developed by Morse, Smale, and others in the 20th Century into a powerful tool for the topological analysis of manifolds.

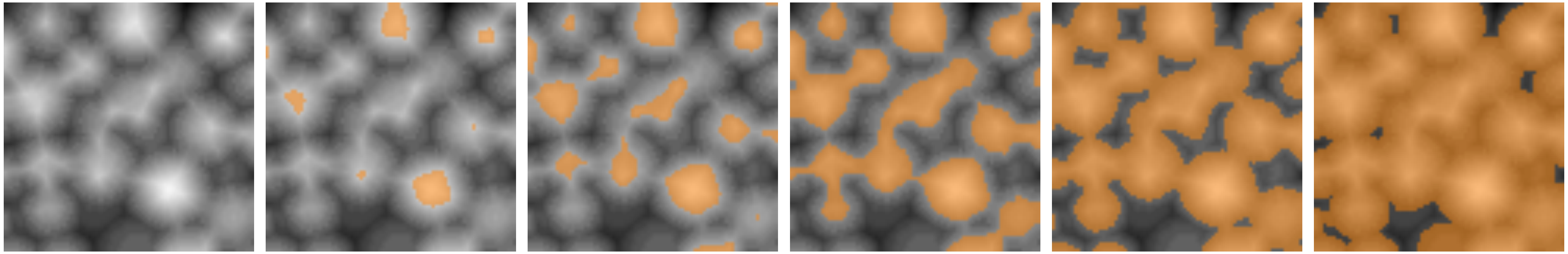

white is low

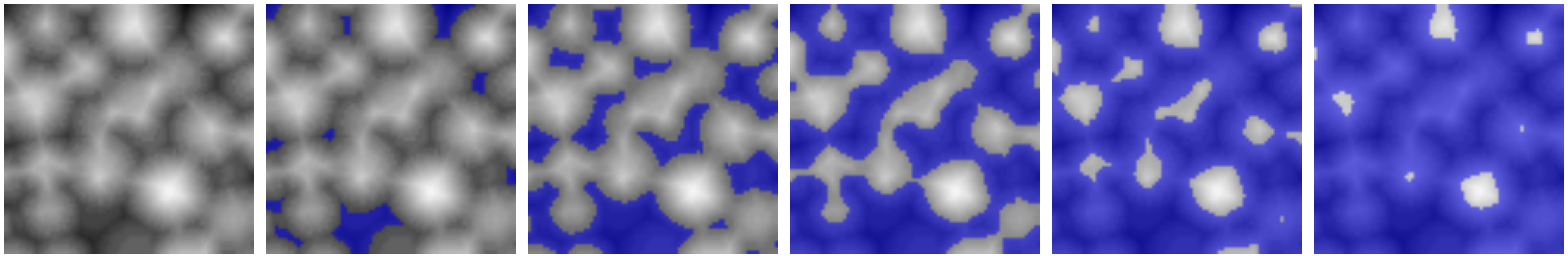

black is low

The Morse chain complex

M_i is the set of index-i critical points.

Gradient flow lines determine adjacencies and the boundary operator, d: M_i to M_{i-1}

This (abstract) chain complex has the same homology as the simplicial homology of the domain.

The filtration orders the critical points by their grey-value

Persistent homology pairs an index-i critical point that creates a cycle with the index-$(i+1)$ critical point that fills in that cycle.

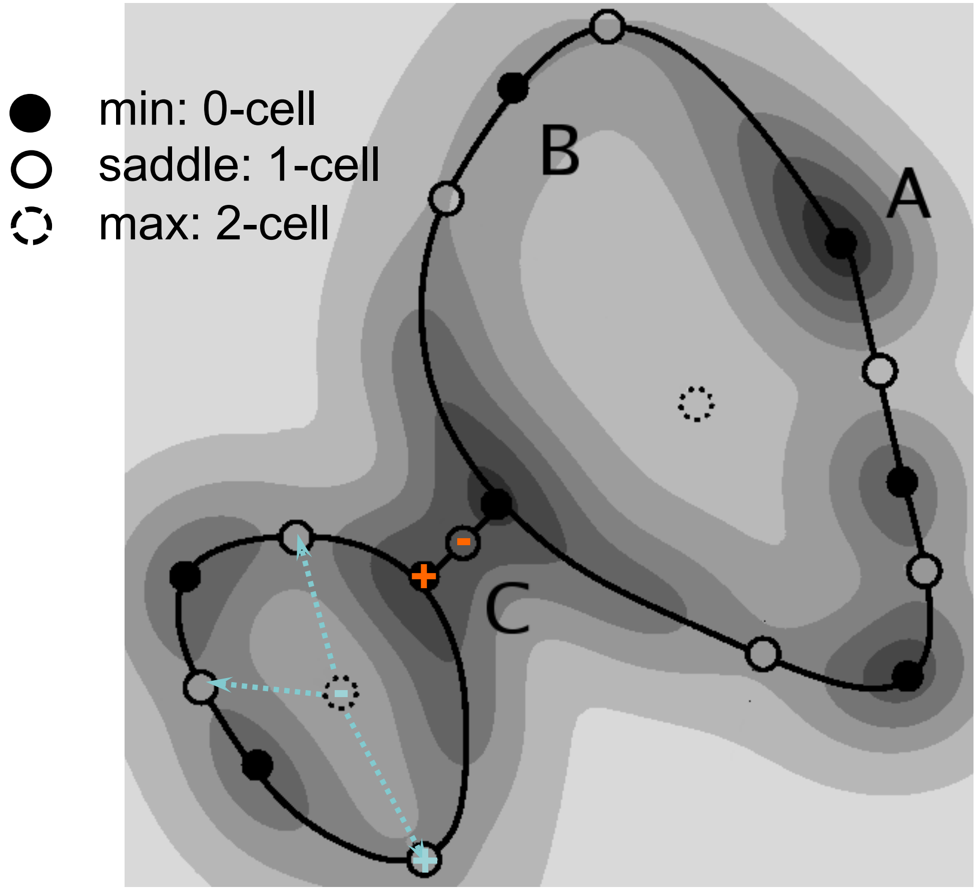

PD0 (b,d) = (1.1,1.5)
PD1 (b,d) = (3.6, 4.5)

Sandstones (pore space)

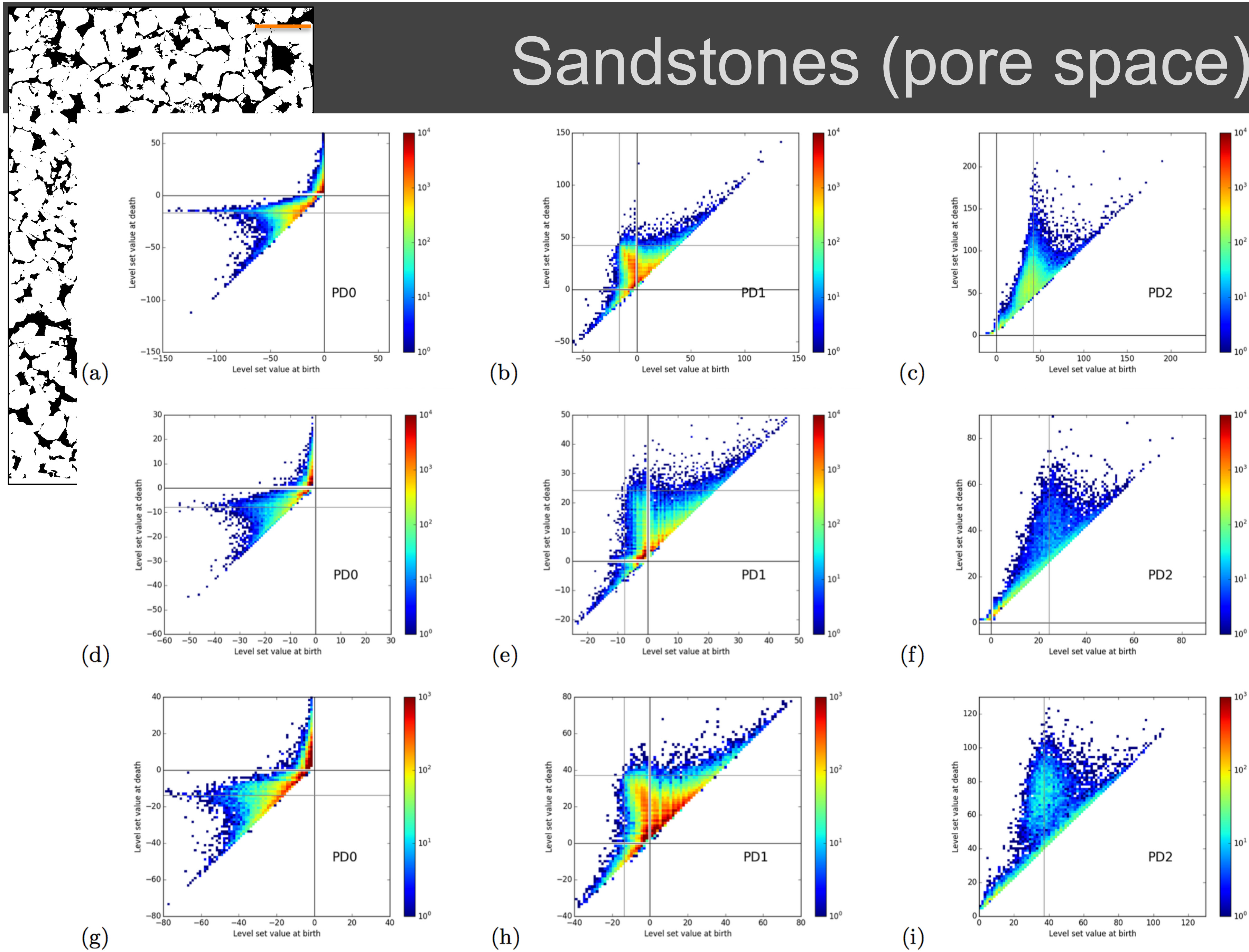

Some observations…

PD0 births measure pore size as radius of max inscribed sphere.

PD0 deaths give the pore-pore throat radius (1-saddles in dist func).

Number of PD1 pairs with b<0, d>0 is the genus of the pore space.

PD1 pairs with birth and death the same sign signal highly non-convex pores or grains.

Symmetry in PD1 and PD0-PD2 duality signals a balance between pore and grain phases

PD2 measures geometry of grains: death values are radii of maximally inscribed spheres.

Appearance of the critical percolating sphere radius as an important length scale in PDs.

Percolation and persistence

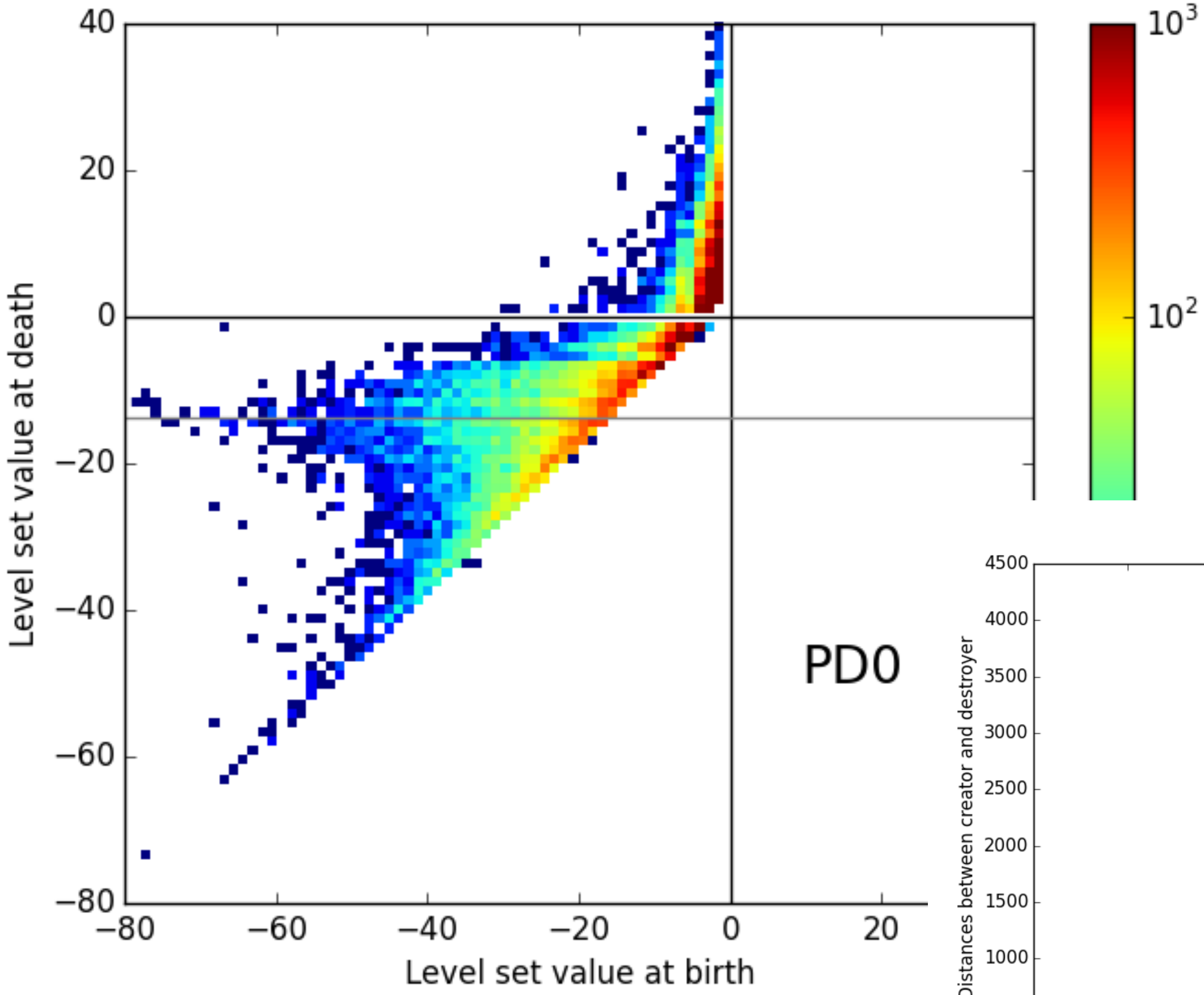

distances between locations of birth, death critical points vs. death value

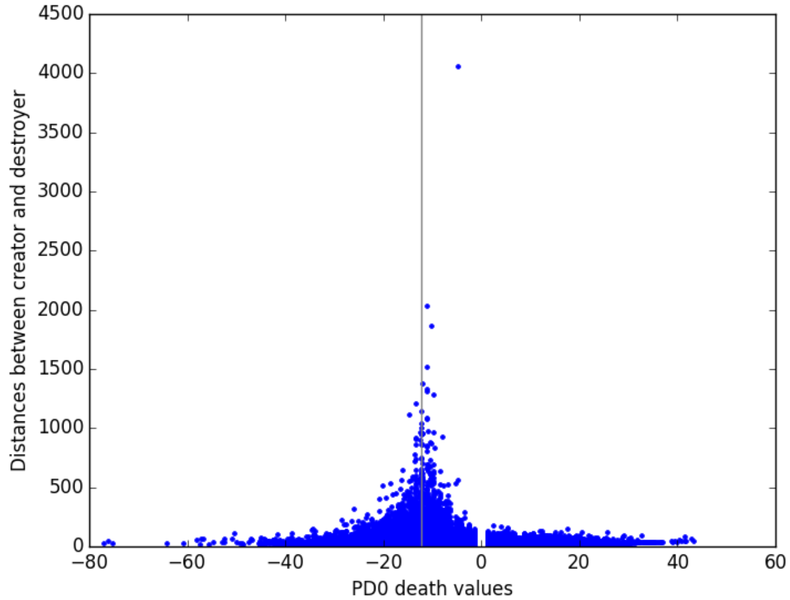

Percolation and persistence

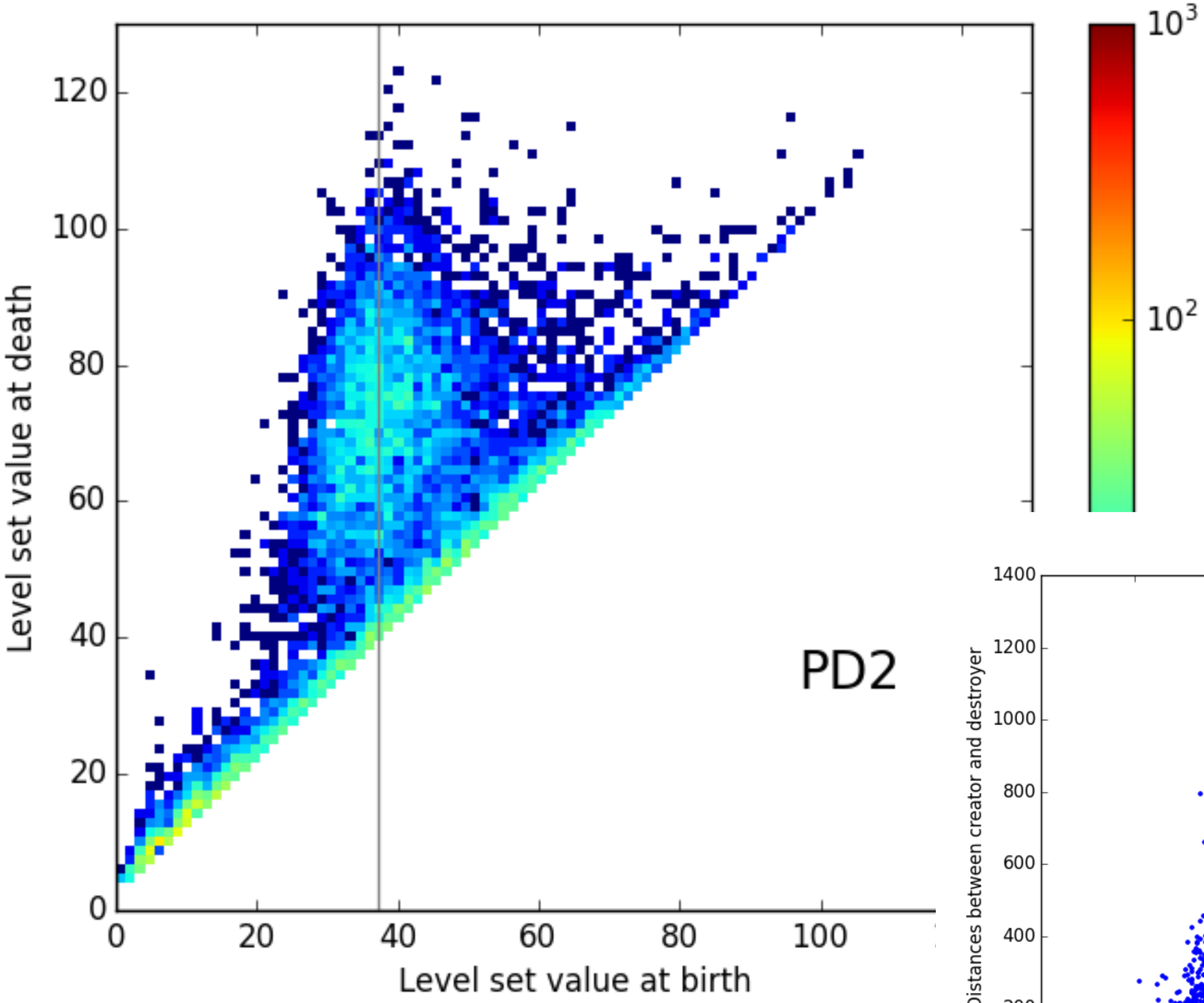

dist(x(birth) – x(death))
vs birth.

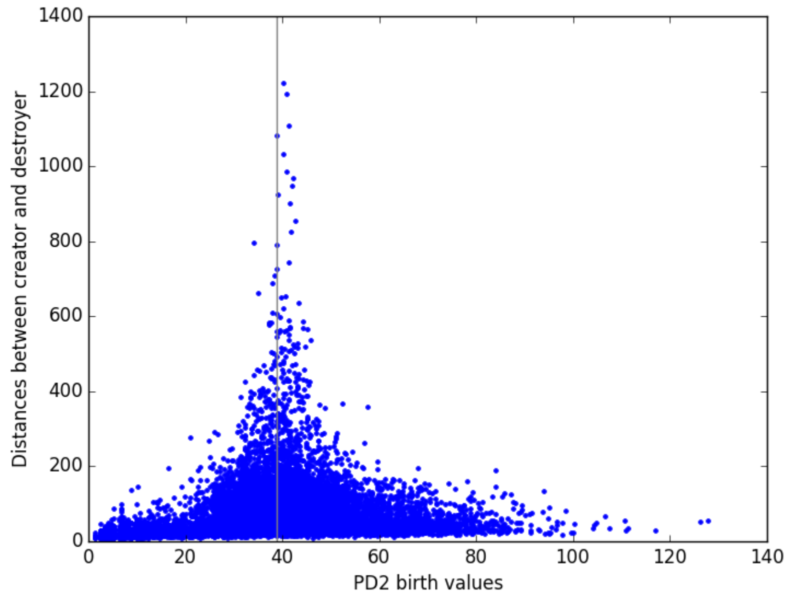

Percolation and persistence

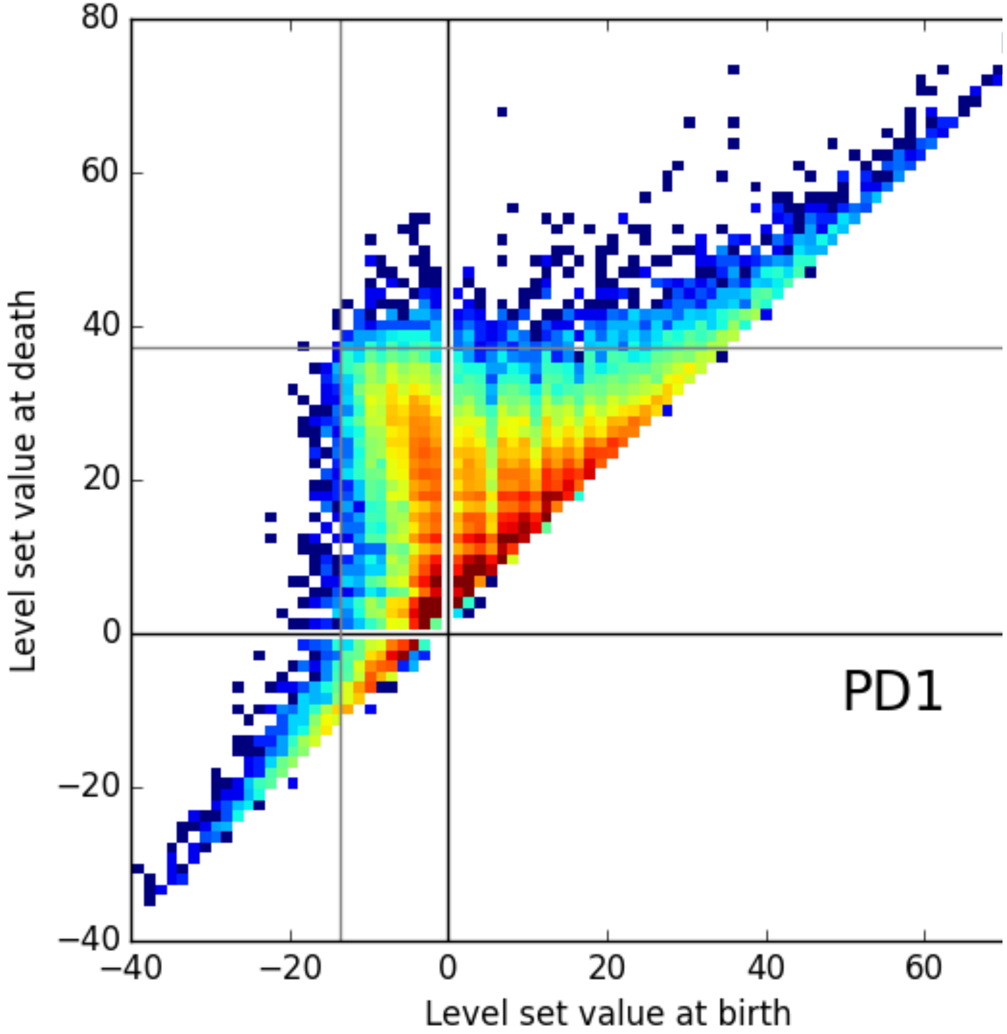

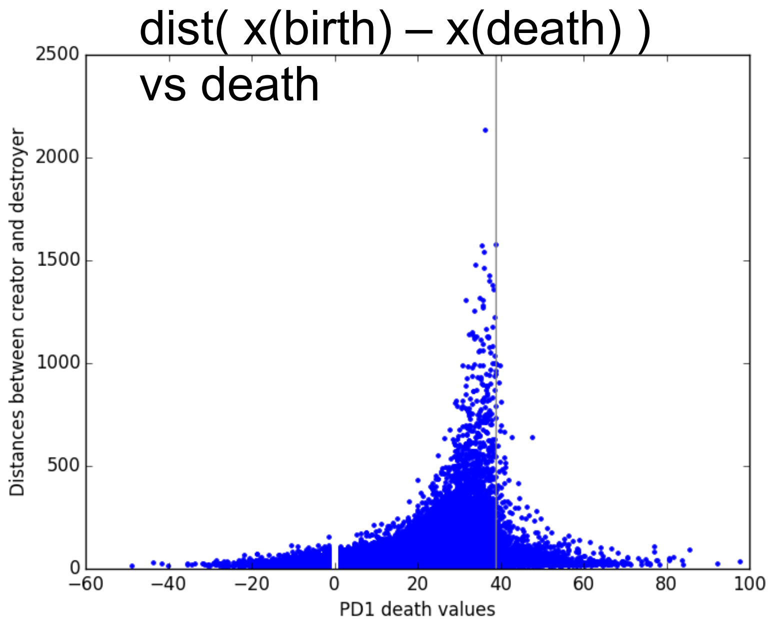

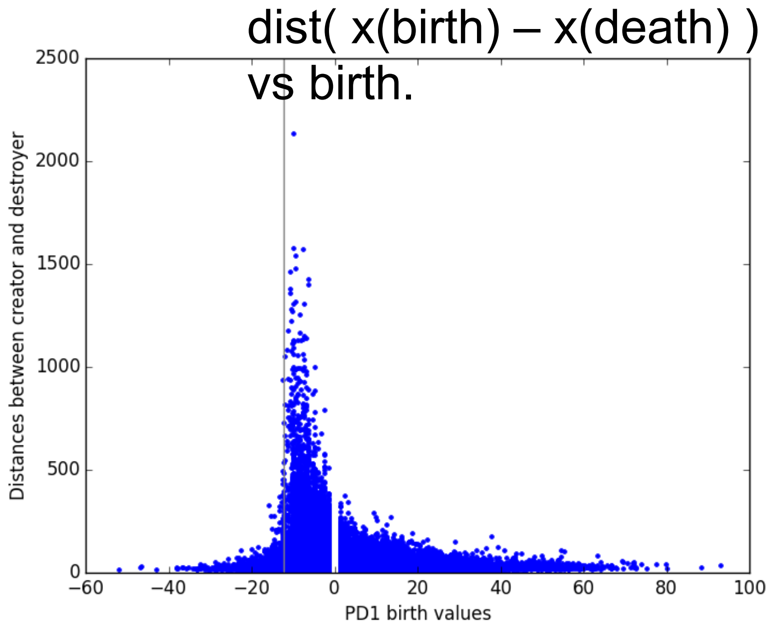

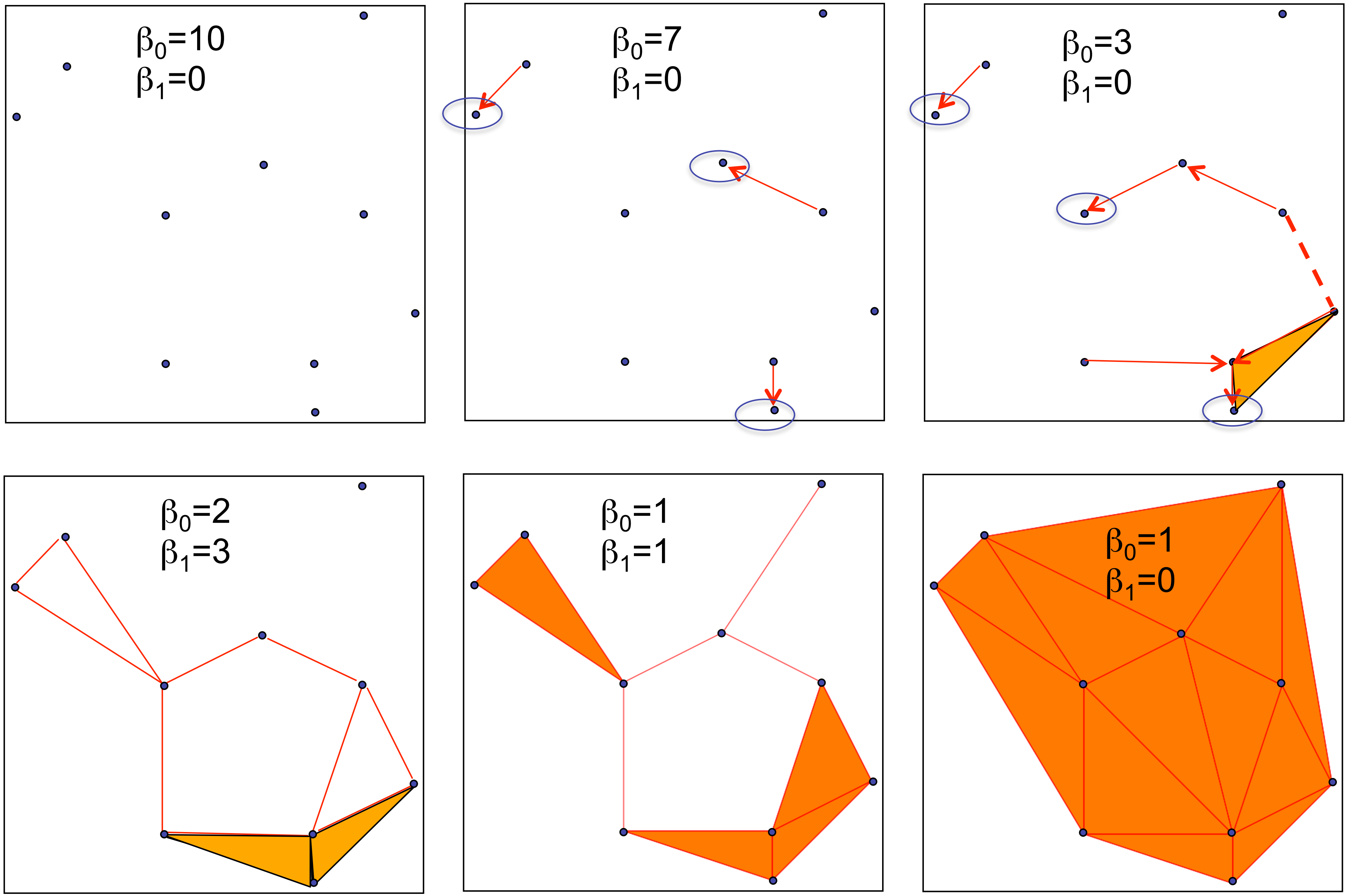

β_0=10
β_1=0
β_0=7
β_1=0
β_0=3
β_1=0
β_0=2
β_1=3
β_0=1
β_1=1
β_0=1
β_1=0